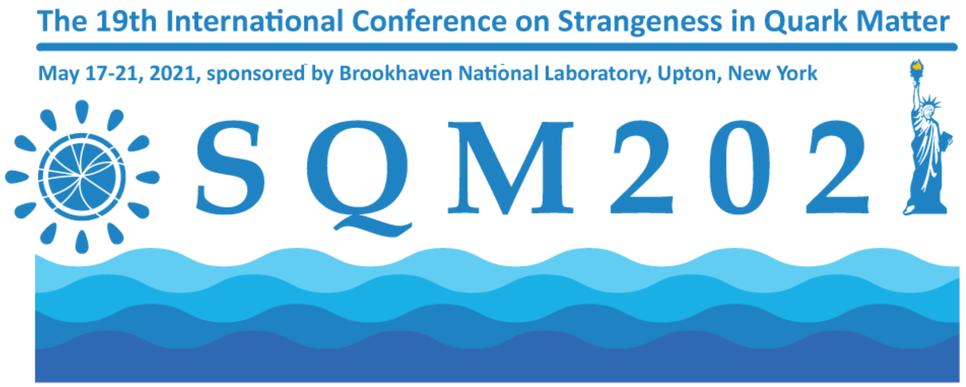

Momentum and multiplicity dependence of strangeness and nuclei production

Alberto Caliva'

May 18, 2021

GSI Helmholtzzentrum für Schwerionenforschung GmbH

UNIVERSITÄT HEIDELBERG
ZUKUNFT SEIT 1386

Introduction

(Multi)strange hadron production:

- Strangeness enhancement
- Phenomenological description of strange hadron production
- Recent results on strangeness production in small collision systems

Light (hyper)nuclei production:

- Phenomenological models describing light nuclei production in high-energy hadronic collisions
- Results on light nuclei from RHIC and LHC
- Hypernuclei production and their structure

(Multi-)strange hadron production

Strangeness enhancement vs. multiplicity

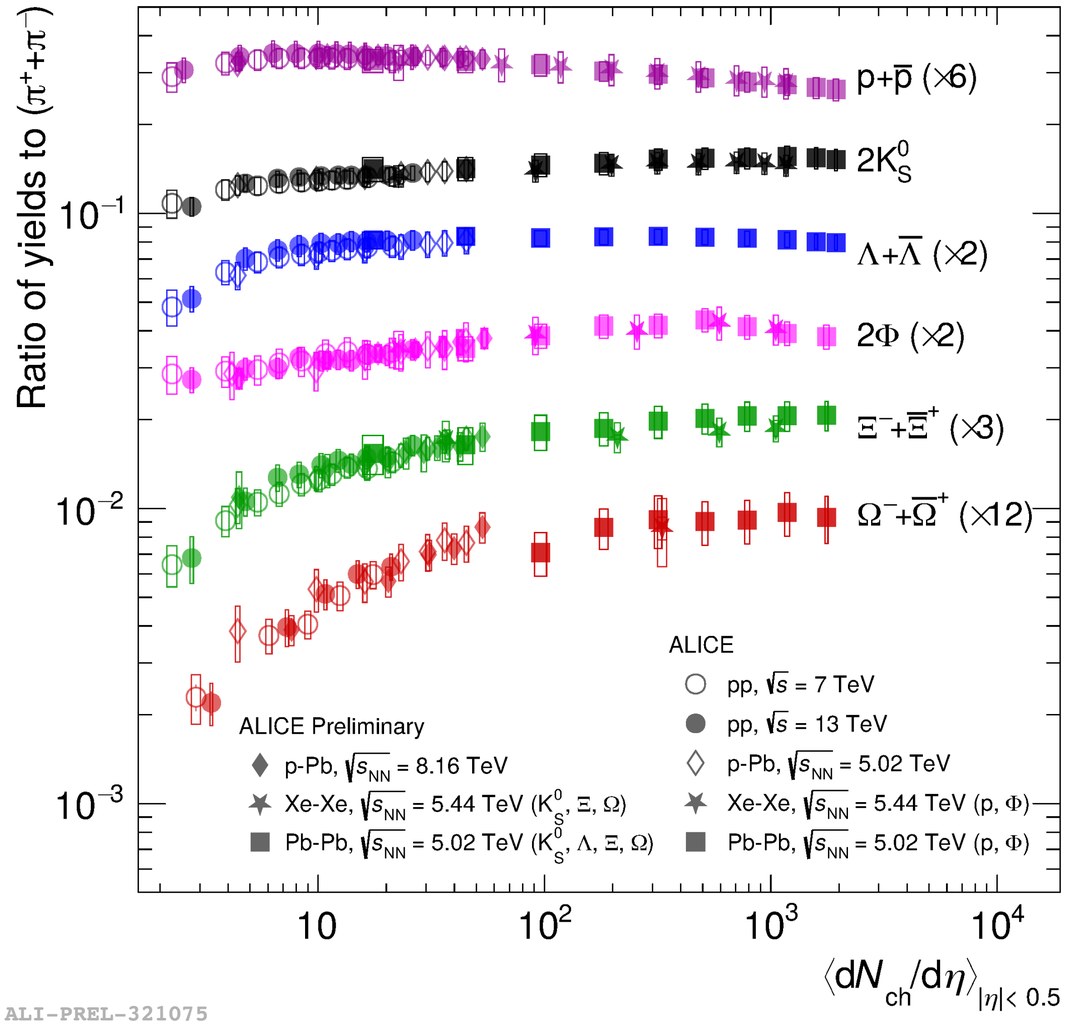

Ratio of (multi-)strange hadron yields and pion yields:

- Smooth evolution with multiplicity across different collision systems and energies
- Significant rise at low multiplicity ($dN_{ch}/d\eta \lesssim 50$) followed by saturation
- Larger increase for hadrons with larger strangeness content

Different phenomenological models are used to describe this effect

→ not fully understood

Nature Phys. 13, 535–539 (2017)

Eur. Phys. J. C 80, 167 (2020)

Canonical suppression

Phys. Rev. C 100, 054906 (2019)

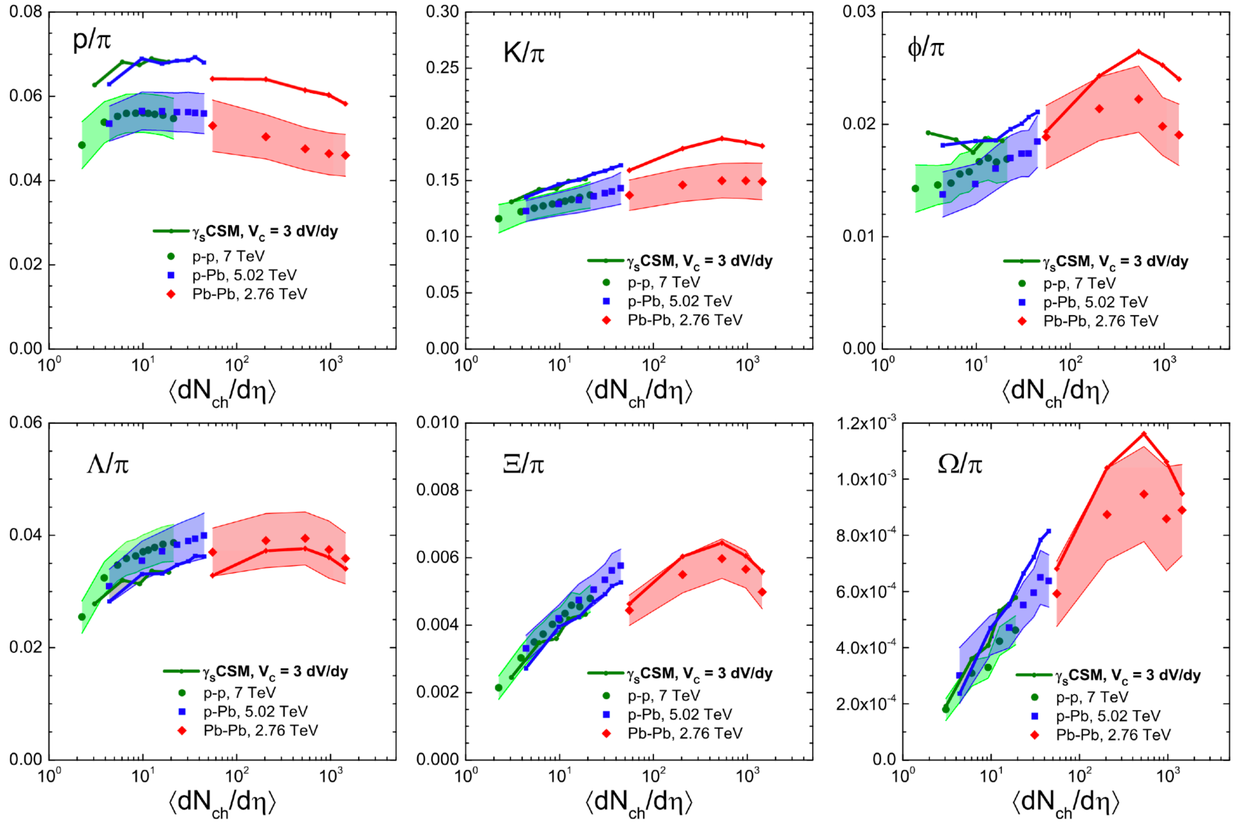

Canonical Statistical Model (CSM):

Multiplicity dependence of strange hadron to pion ratio emerges from exact conservation of charges in the correlation volume V_c (S=Q=B=0)

- **Strangeness suppression** at low multiplicity

Recent developments (γ_S—CSM) include:

- Multiplicity-dependent T_{chem}
- Incomplete chemical equilibration described by a multiplicity-dependent strangeness saturation parameter γ_S

Good description of the available data except for p/π ratio

- 2σ discrepancy at all multiplicities

Strangeness suppression at low energy

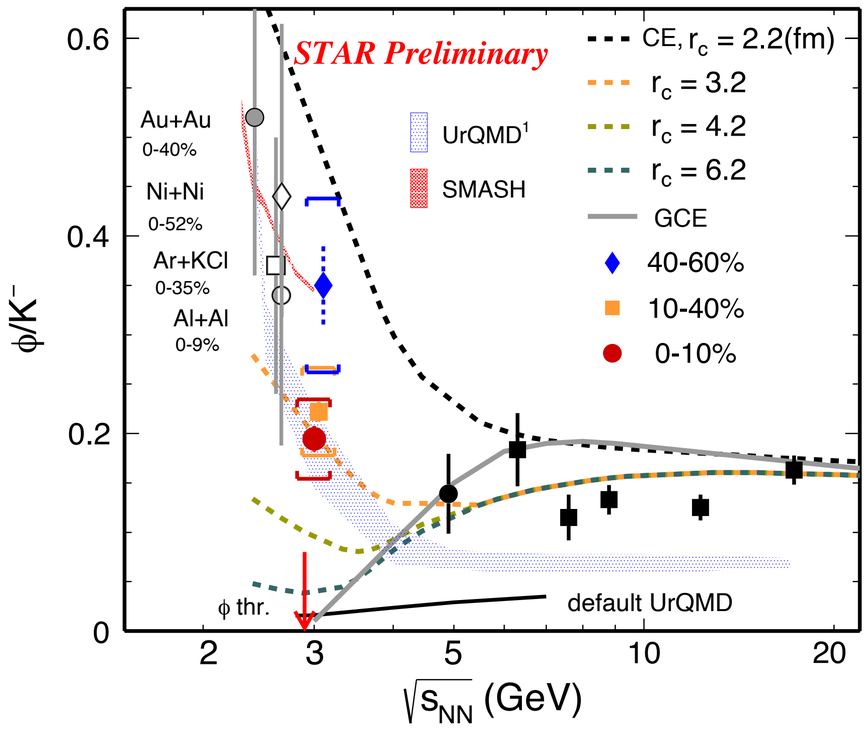

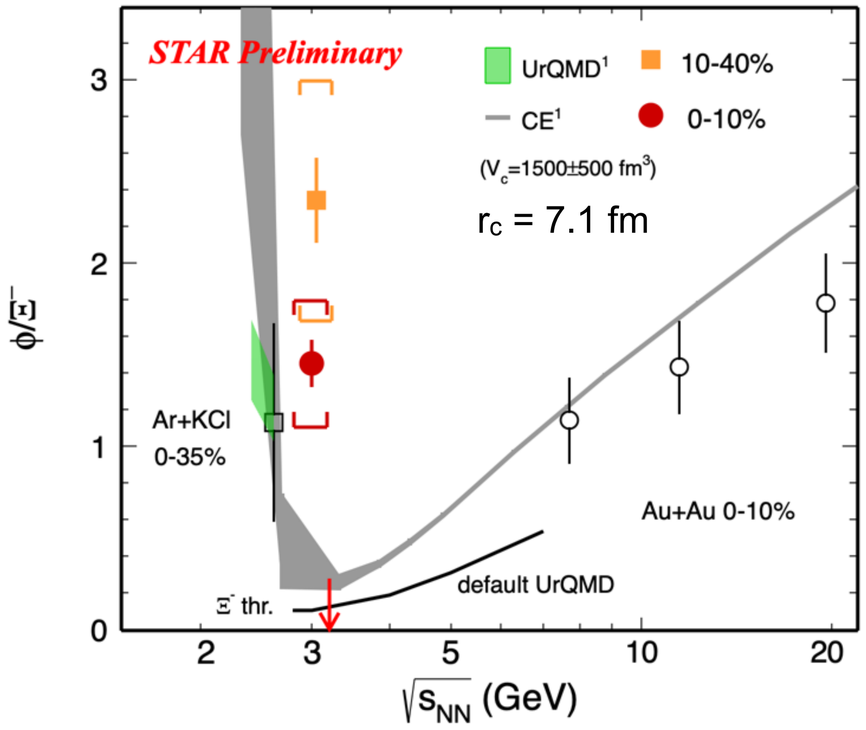

A. Andronic *et al.*,
Nucl. Phys. A 772 (2006) 167-199

J. Cleymans *et al.*,
Phys. Lett. B 603 (2004) 146-151

ϕ/K and ϕ/Ξ ratios vs. $\sqrt{s_{\mathrm{NN}}}$:

- interplay between $\sqrt{s_{\mathrm{NN}}}$ dependence of T and μ_{B} and canonical suppression → dominant for $\sqrt{s_{\mathrm{NN}}}$ < 3–4 GeV
- stronger suppression for fixed $\sqrt{s_{\mathrm{NN}}}$ going from central to peripheral collisions
- stronger suppression for hadrons with larger strangeness content (ϕ/Ξ > ϕ/K)

Core-corona model

Phys. Rev. C 101, 024912 (2020)

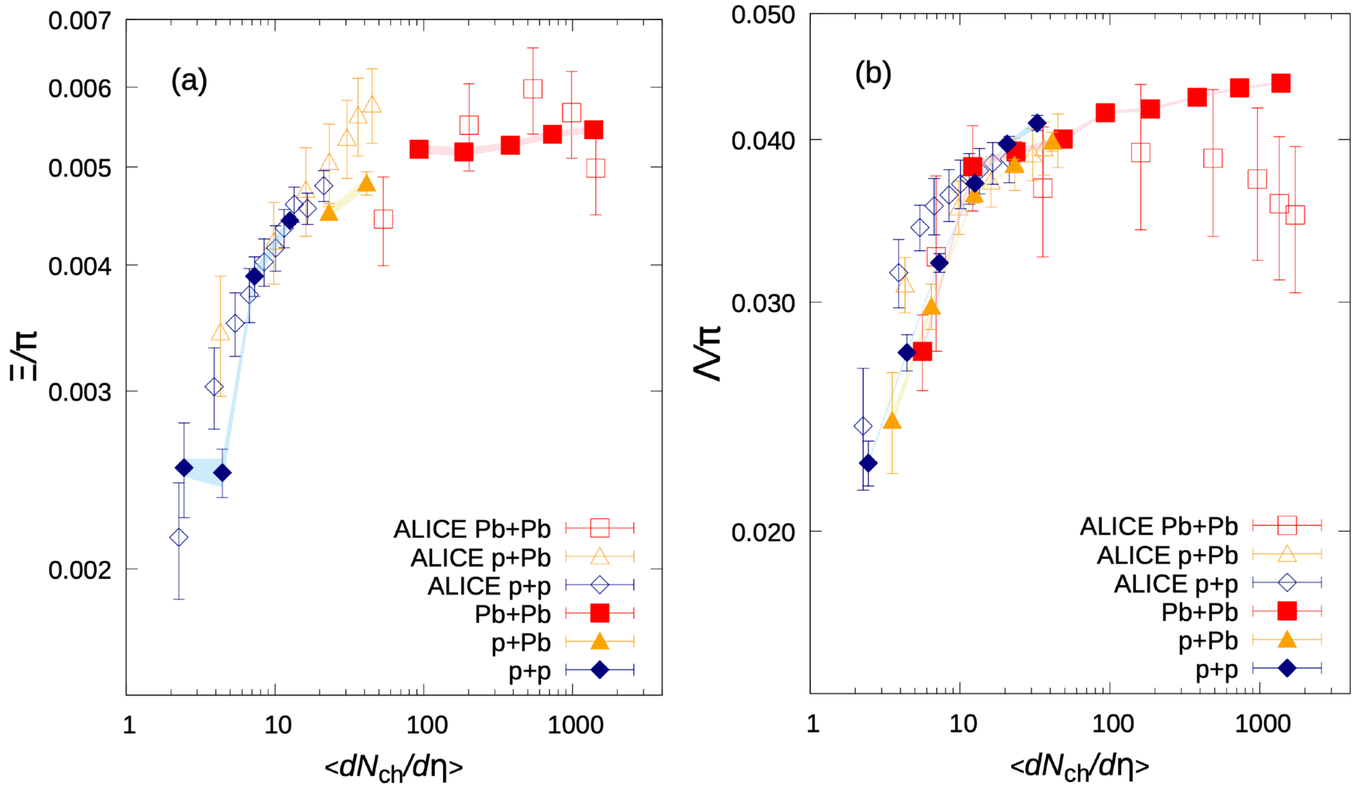

Hadron production from a two-component (core-corona) model:

$$\left\langle \frac{dN_i}{dy} \right\rangle = \left\langle \frac{dN_i}{dy} \right\rangle_{\text{core}} + \left\langle \frac{dN_i}{dy} \right\rangle_{\text{corona}}$$

Core: high-density, QGP in thermal and chemical eq.

Corona: low-density, string fragmentation

Smooth evolution from string fragmentation regime in pp to statistical hadronization in AA collisions:

- increase of relative contribution from the “core” with increasing multiplicity

Ropes hadronization

Strangeness enhancement from **rope hadronization + color reconnection**

- Mechanism based on the Lund string fragmentation model

Ropes: overlapping strings in high-energy collisions (MPI)

→ higher string tension

high energy density in overlap region leads transverse expansion of hadronizing strings (*string stoving*)

→ effects similar to a collective expansion

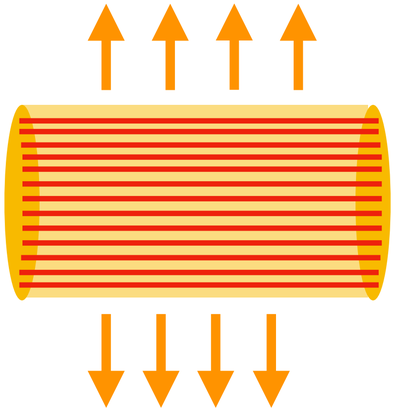

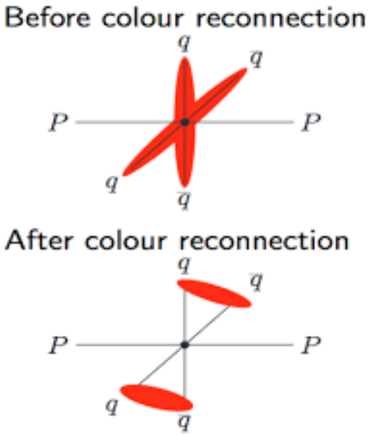

Color reconnection: re-arrangement of color strings

Phys. Rev. D 100, 074023 (2019)

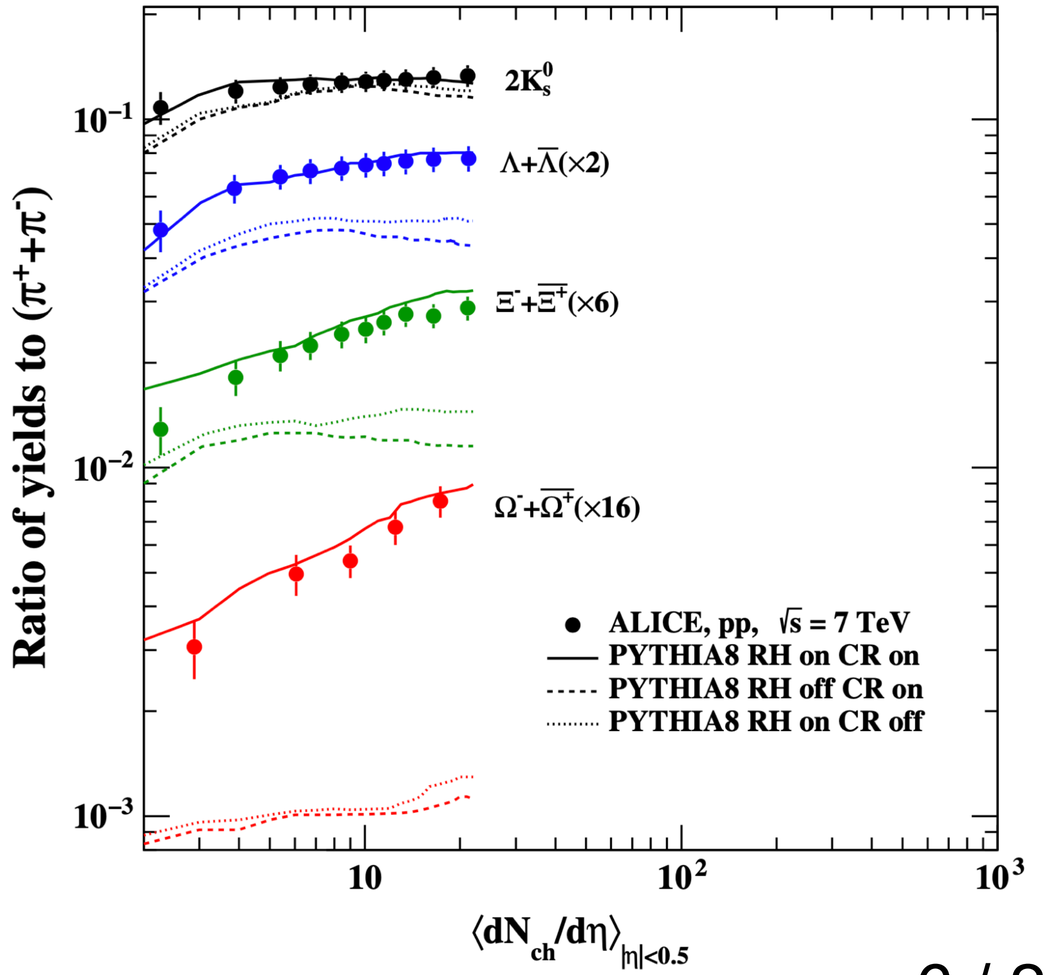

Strangeness vs. effective energy

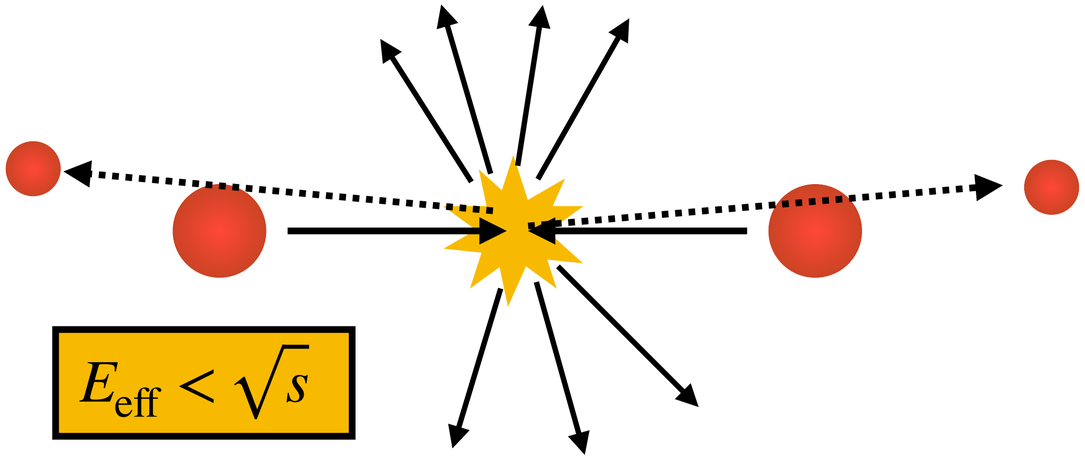

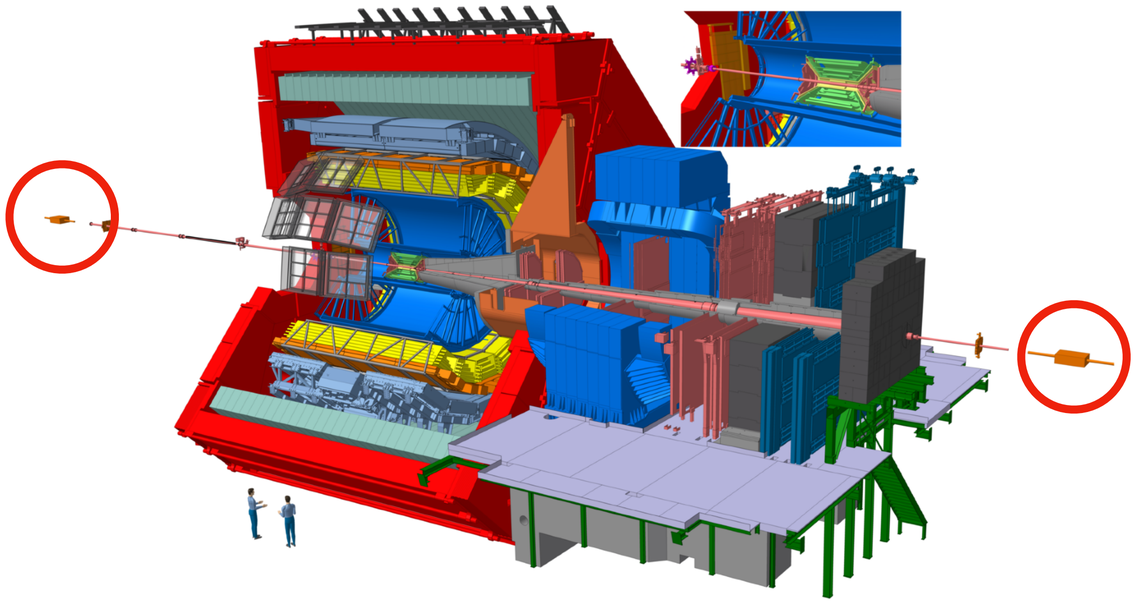

Forward emission of baryons in pp collisions, called *leading effect* **(Phys. Lett. B 92 (1980) 367)**:

- Fraction of available energy carried away

This reduces the effective energy for particle production at midrapidity: $E_{\text{eff}} < \sqrt{s}$

Does strangeness production depend on effective energy?

Energy of “leading baryon” can be measured using the Zero-Degree Calorimeters (ZDC)

$$E_{\text{eff}} = \sqrt{s} - E_{\text{ZDC}}$$

Strangeness vs. effective energy

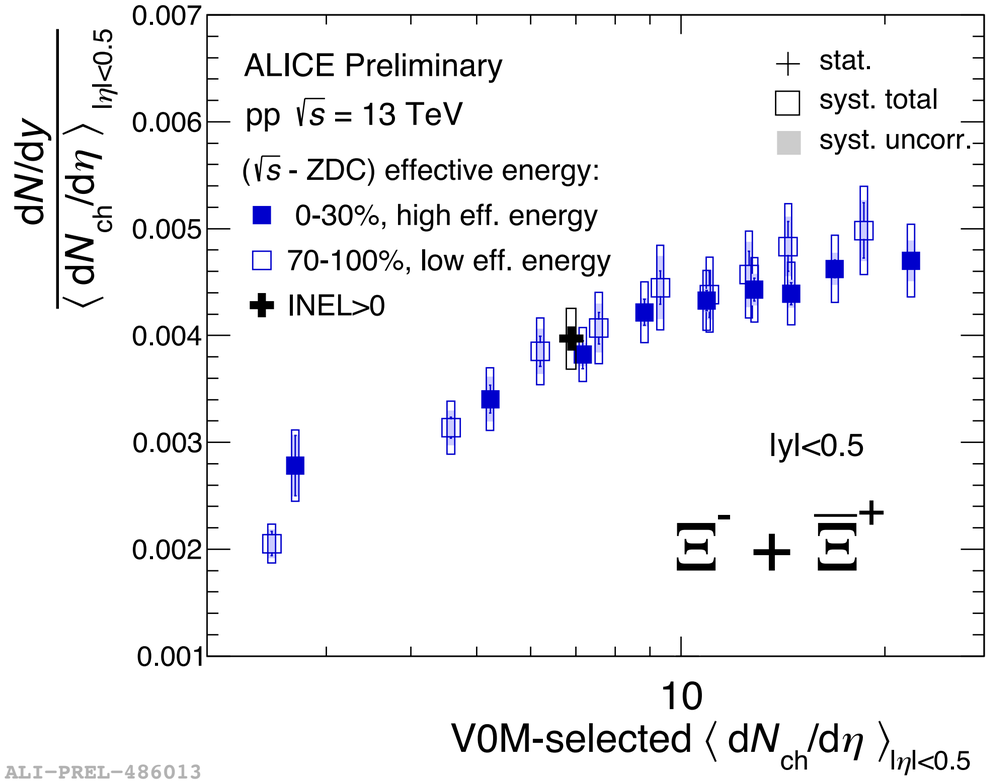

ALI-PREL-486013

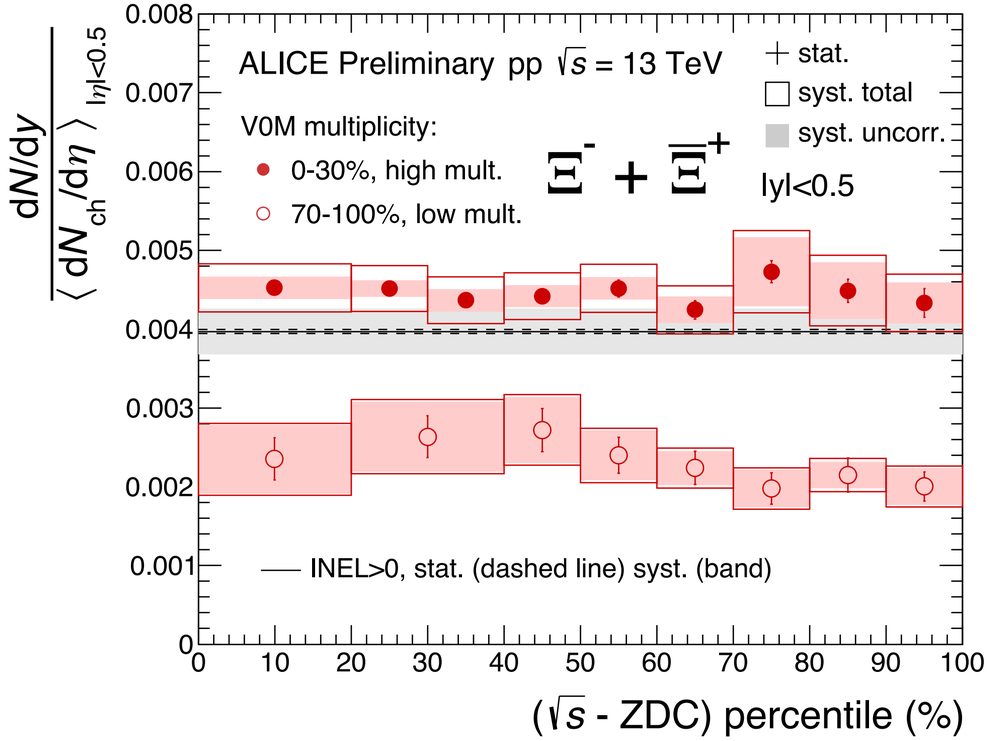

ALI-PREL-486021

$\sqrt{s} - E_{\mathrm{ZDC}}$ percentile classes:

- 0–20%: low forward energy deposit (large E_{eff})
- 90–100%: large forward energy deposit (low E_{eff})

Strangeness production seems to be independent of the effective energy and is mainly driven by the final-state multiplicity

Strangeness in and out of jets

arXiv:2105.04890 [nucl-ex], submitted to PLB

Jet region:
R ≤ 0.4

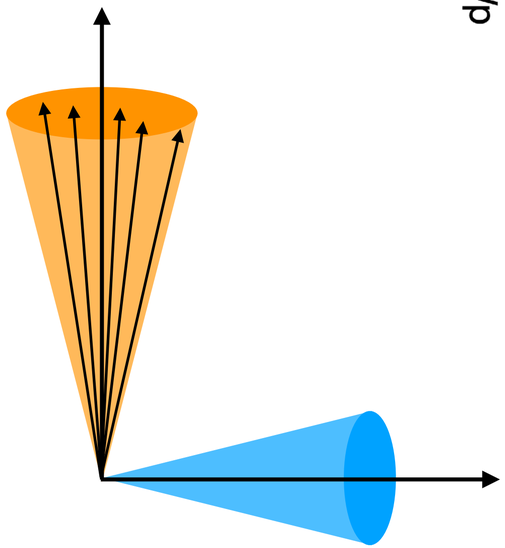

Underlying event:
Perpendicular cone

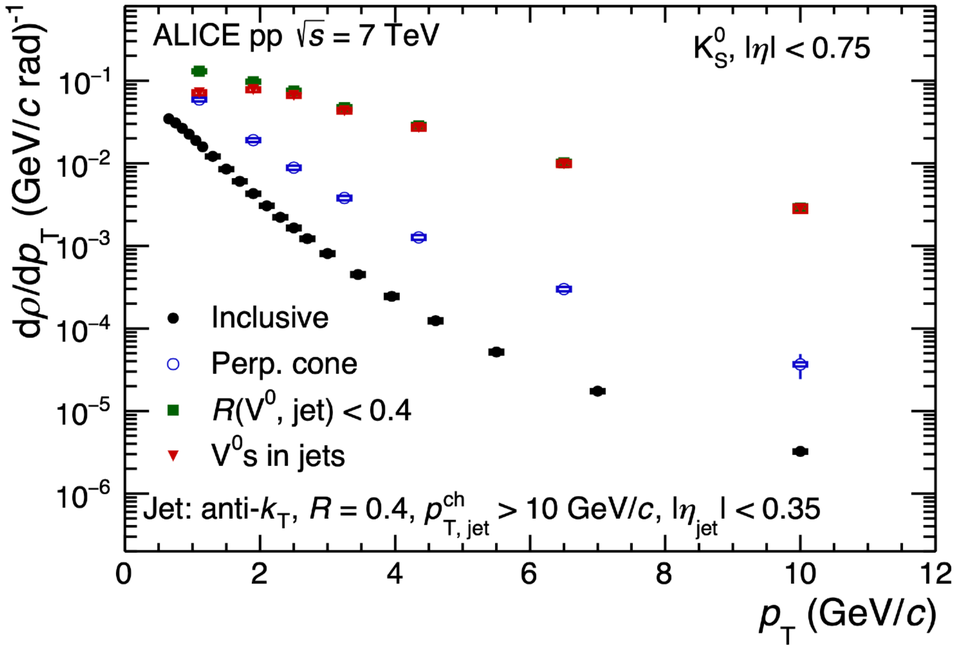

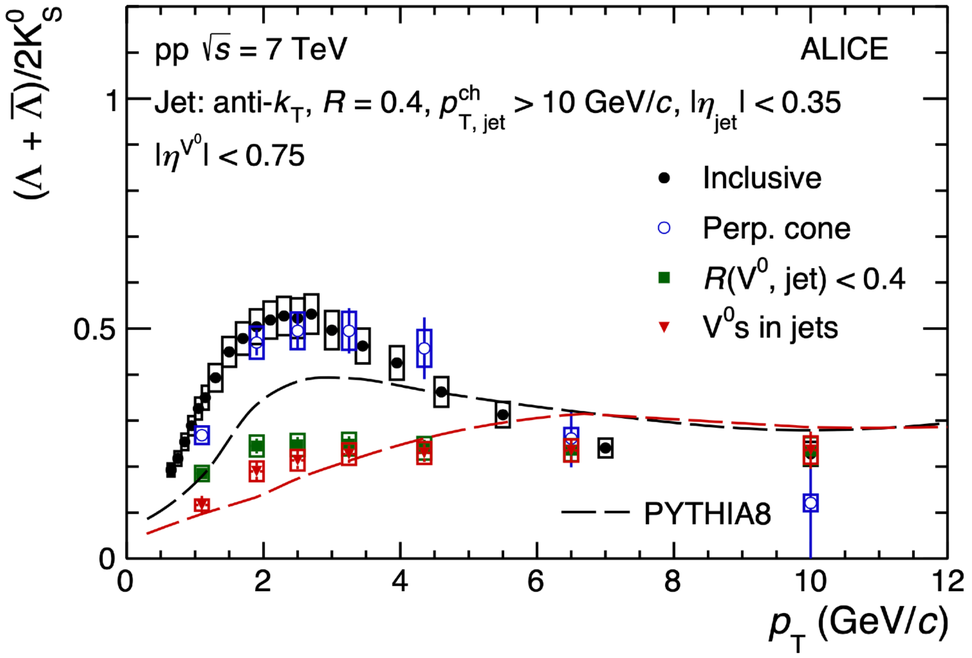

p_T spectra in jet are harder than in the UE

- Different p_T dependence of Λ/K^0_S in jet and UE: different production mechanisms?
- Inclusive Λ/K^0_S consistent with UE: small relative contribution from jet to strangeness production

Strangeness in and out of jets

Strangeness production in and out of jet via two-particle correlation method:

- Trigger primary particle as proxy for the jet (highest p_T and p_T > 3 GeV/c)
- $\Delta\eta$ and $\Delta\phi$ of strange hadron wrt trigger particle define in-jet and out-of-jet regions

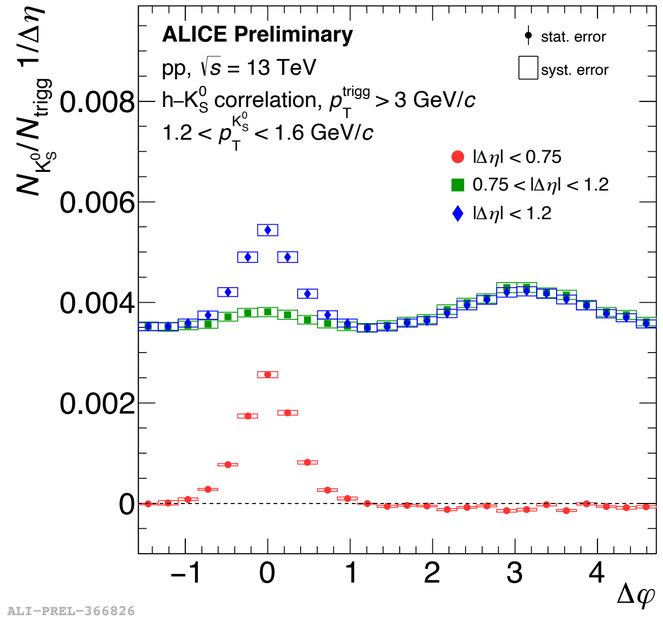

Ξ in jet

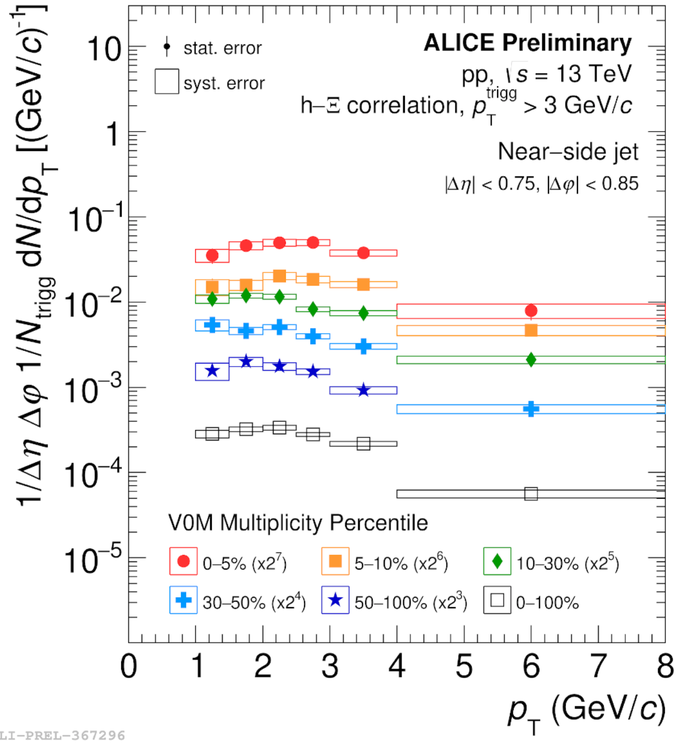

Ξ out of jet

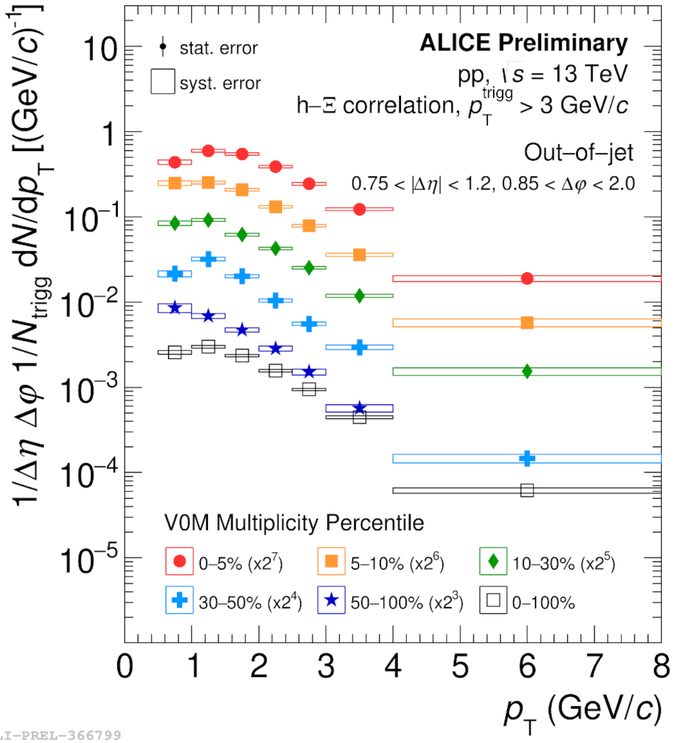

K^0_S and Ξ production in and out of jet are studied in different event multiplicity classes

Strangeness in and out of jets

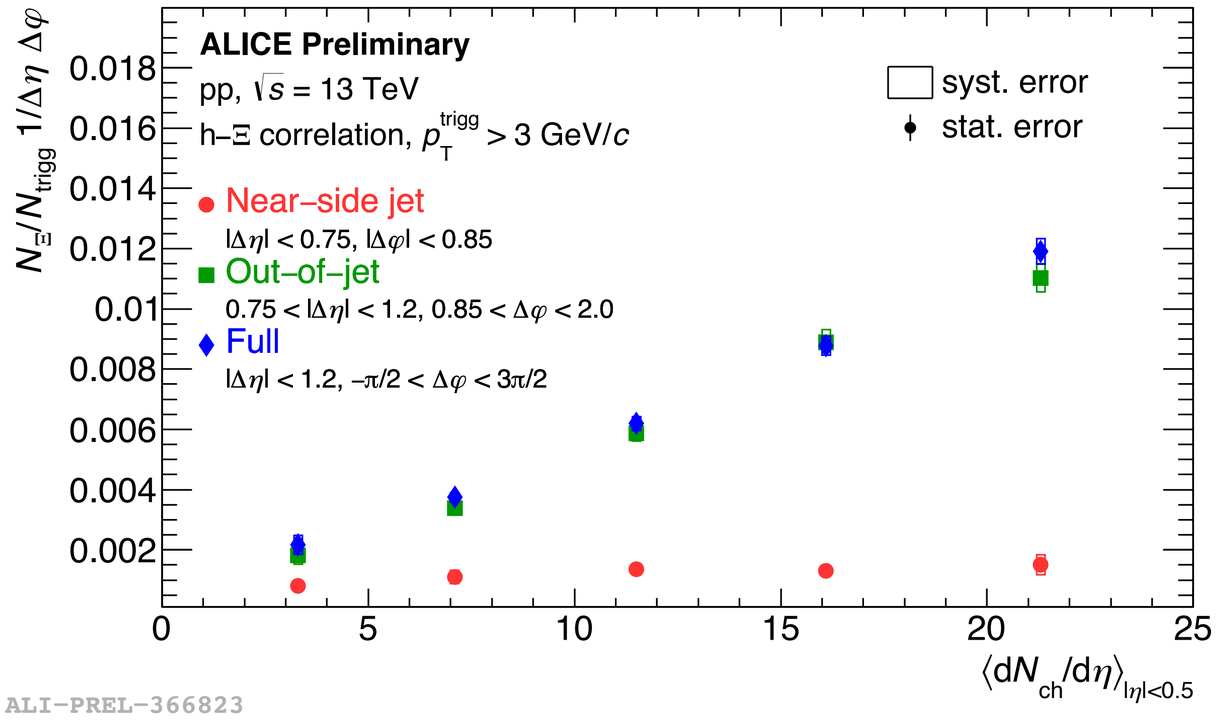

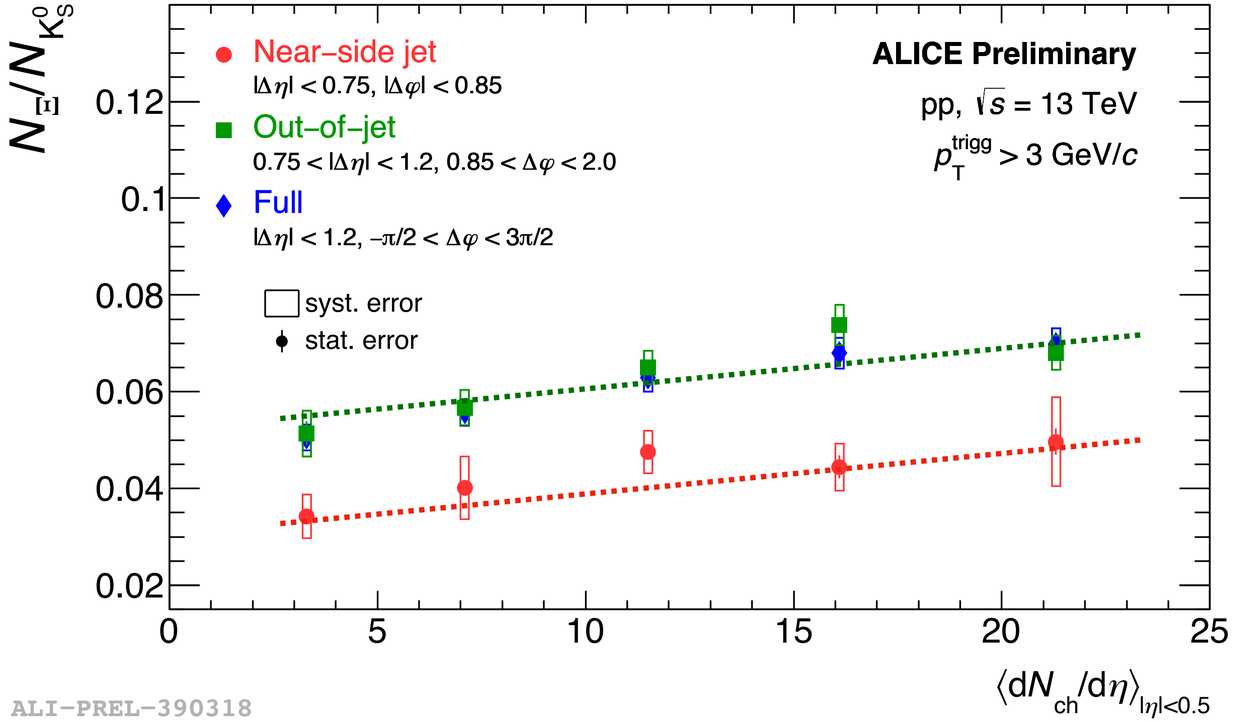

Yield of strange hadrons in the UE rises faster with multiplicity than in the jet region

Inclusive Ξ/K^0_S vs. multiplicity consistent with that measured in the UE

- Smaller relative contribution of strangeness production in jets
- Strangeness enhancement both in and out-of-jet on two different levels

Light (hyper)nuclei production

Light (hyper)nuclei production

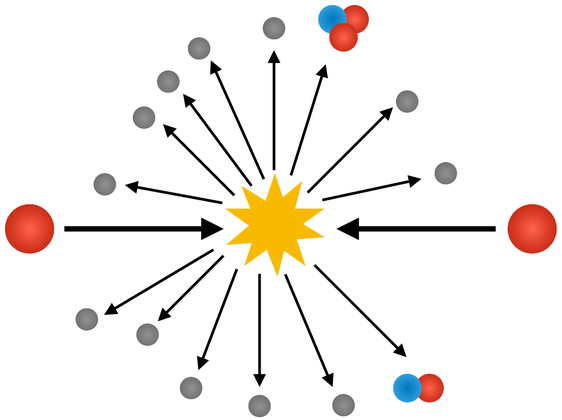

Phys. Lett. B 754 (2016) 6–10

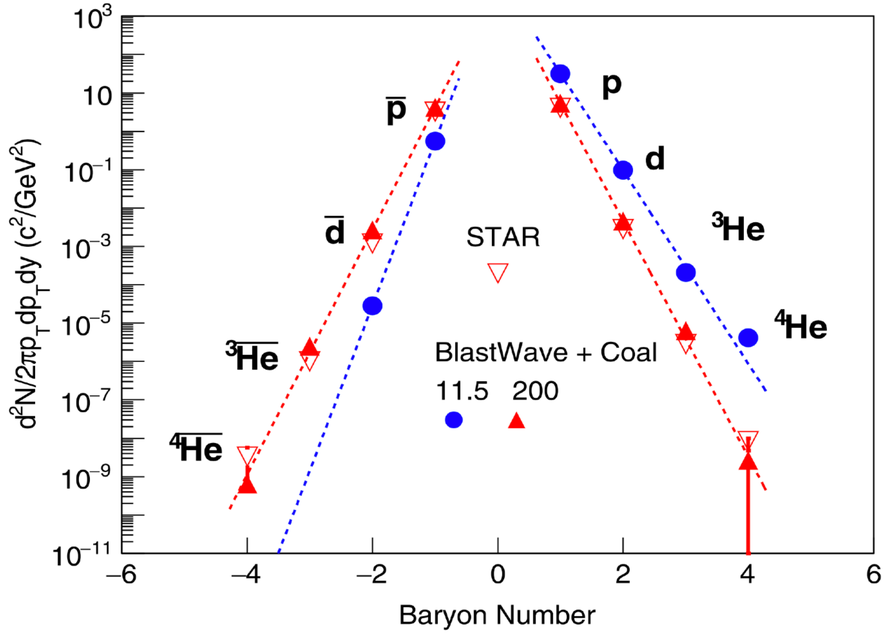

Nucl. Phys. A 971 (2018) 1-20

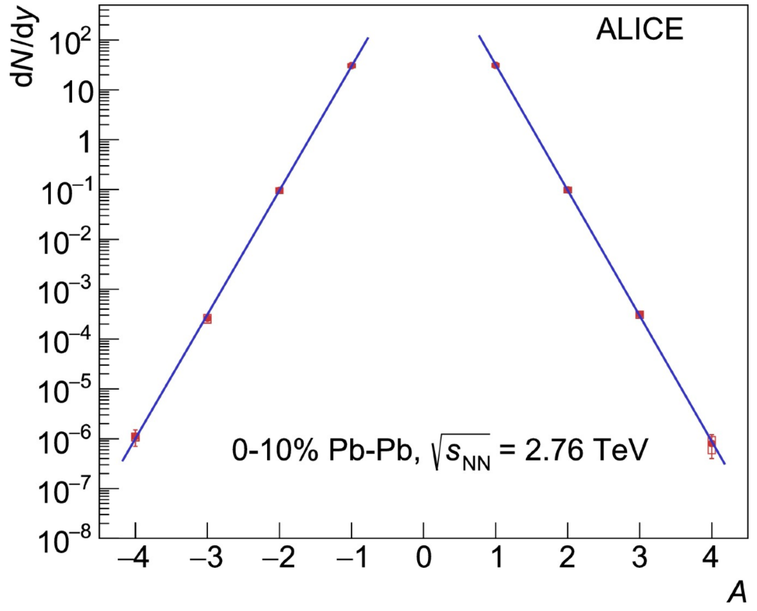

Production mechanism of light (anti)(hyper)nuclei in high-energy hadronic collisions still under debate

Different phenomenological models typically used:

- Statistical hadronization model
- Coalescence model
- Hybrid models: hydro + (coalescence) afterburners

Statistical hadronization model

A. Andronic *et al.*, Nature vol. 561, p. 321–330 (2018)

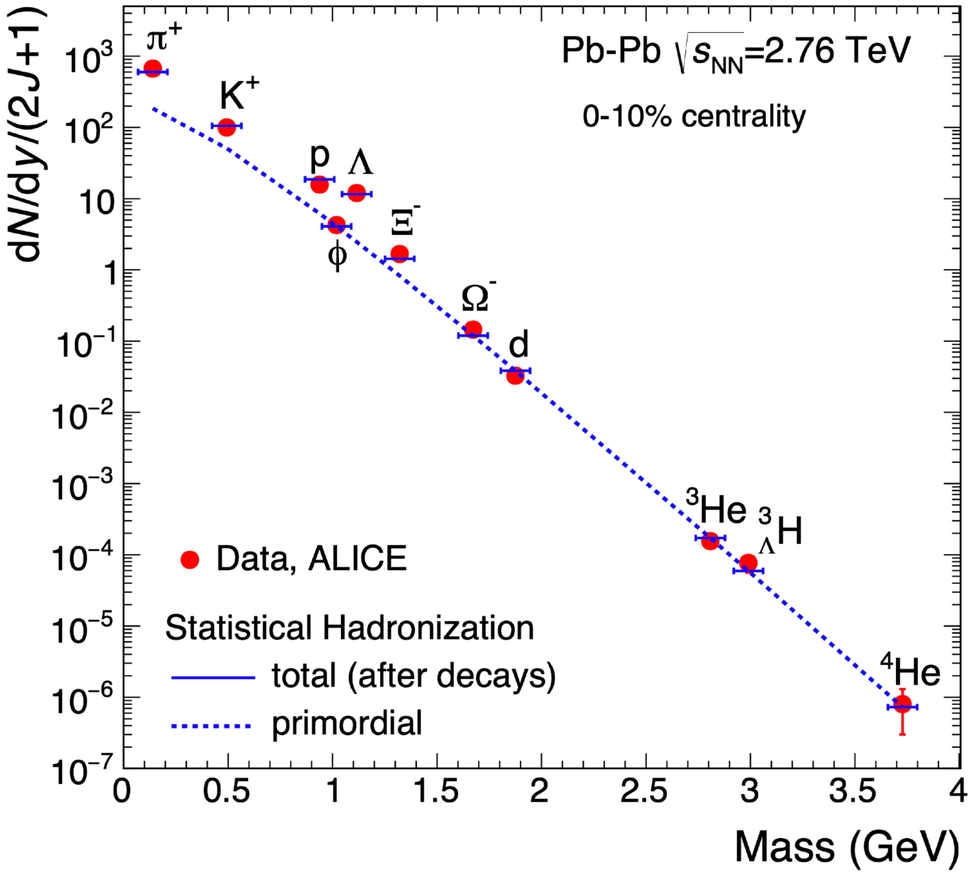

Hadron yields at chemical freeze-out calculated using the hadronic partition function:

$$n_{\mathrm{i}} = -\frac{T}{V}\frac{\partial\, ln(Z_{\mathrm{i}})}{\partial\mu} = \frac{g_{\mathrm{i}}}{2\pi^2}\int_0^{\infty}\frac{\mathrm{d}p\; p^2}{\exp[(E_{\mathrm{i}}-\mu_{\mathrm{i}})/T]\pm 1} \rightarrow \frac{\mathrm{d}N_i}{\mathrm{d}y} = n_i\cdot\frac{\mathrm{d}V}{\mathrm{d}y}$$

primordial yields + feed-down from high-mass states

Fit experimental data using 3 free parameters: T_{chem}, V, μ_B

$$T_{\mathrm{chem}} = 156.5 \pm 1.5\ \mathrm{MeV} \rightarrow T_{\mathrm{chem}} \approx T_{\mathrm{pc}}$$

Chemical freeze-out close to phase boundary!

Survival of light nuclei to hot hadron gas: compact (colorless) quark bags

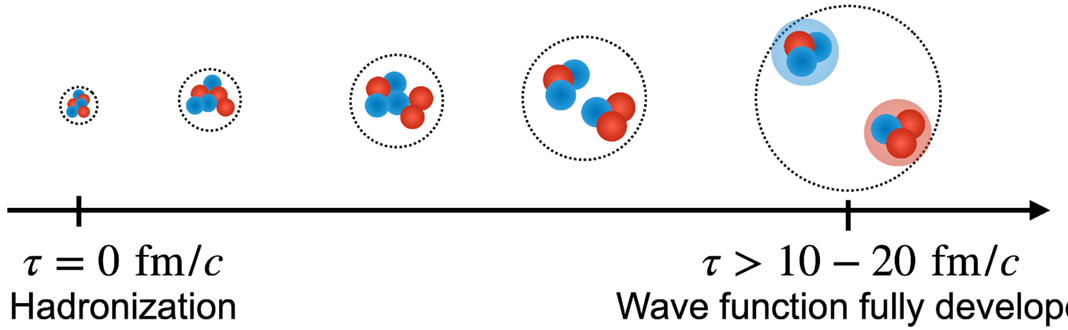

(Simple) coalescence model

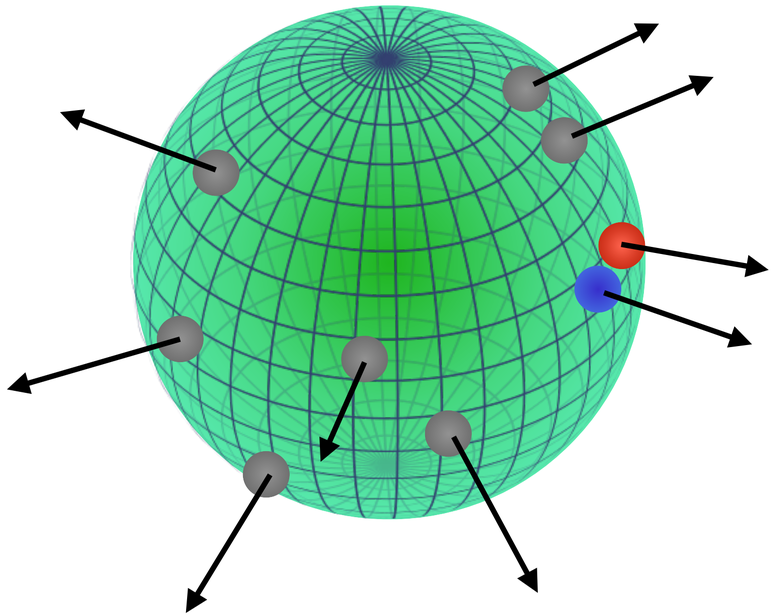

Bound states formed by coalescence of baryons which are close in phase space at kinetic freeze-out

- Baryon(s) need(s) to be off the mass shell for momentum conservation
- Proper spin configuration
- Bound states fully formed after $\tau_{\mathrm{form}} > \hbar / E_{\mathrm{b}}$
  e.g., deuteron (proper) formation time > 100 fm/*c*

J.Kapusta, Phys. Rev. C 21 (1980) 1301

Coalescence probability quantified by the coalescence parameter B_A

$$E_A \frac{d^3N_A}{dp_A^3} = B_A \cdot \left(E_p \frac{d^3N_p}{dp_p^3} \right)^A \qquad p_p = p_A / A$$

Invariant yield of nucleus

Coalescence parameter

Invariant yield of protons

In the simple coalescence model only momentum correlations are considered:

coalescence happens if $\Delta p < p_0$

(Advanced) coalescence model

In the state-of-the-art coalescence implementations and in hybrid approaches:

$$N_A = \underbrace{g_A}_{\text{spin-isospin degeneracy factor}} \cdot \int d^3x_1 \ldots d^3x_A \cdot d^3k_1 \ldots d^3k_A \cdot \underbrace{f_1(x_1, k_1)}_{\text{phase space distributions of (point-like) nucleons taken from hydro + hadronic afterburner}} \cdot \underbrace{f_A(x_A, k_A)}_{\text{phase space distributions of (point-like) nucleons taken from hydro + hadronic afterburner}} \cdot \underbrace{W_A(x_1, \ldots, x_A, k_1, \ldots k_A)}_{\text{Wigner density of the nucleus}}$$

Two alternative Wigner densities typically used in the calculations:

- $W_A = 1 \text{ for } \begin{cases} \Delta x < \Delta x_{max} \\ \Delta p < \Delta p_{max} \end{cases}$
- Gaussian approximation

S. Sombun *et al.*, Phys. Rev. C 99 (2019) 014901

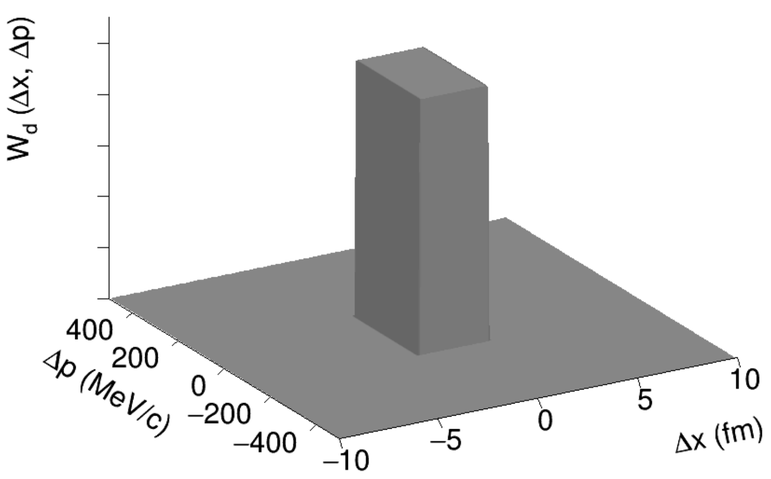

K.Sun *et al.*, Phys. Lett. B 792 (2019) 132-137

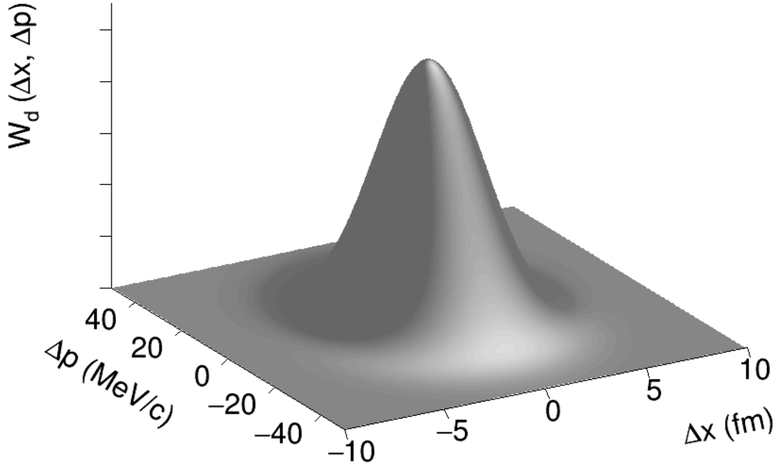

Deuteron p_T spectra vs. coalescence

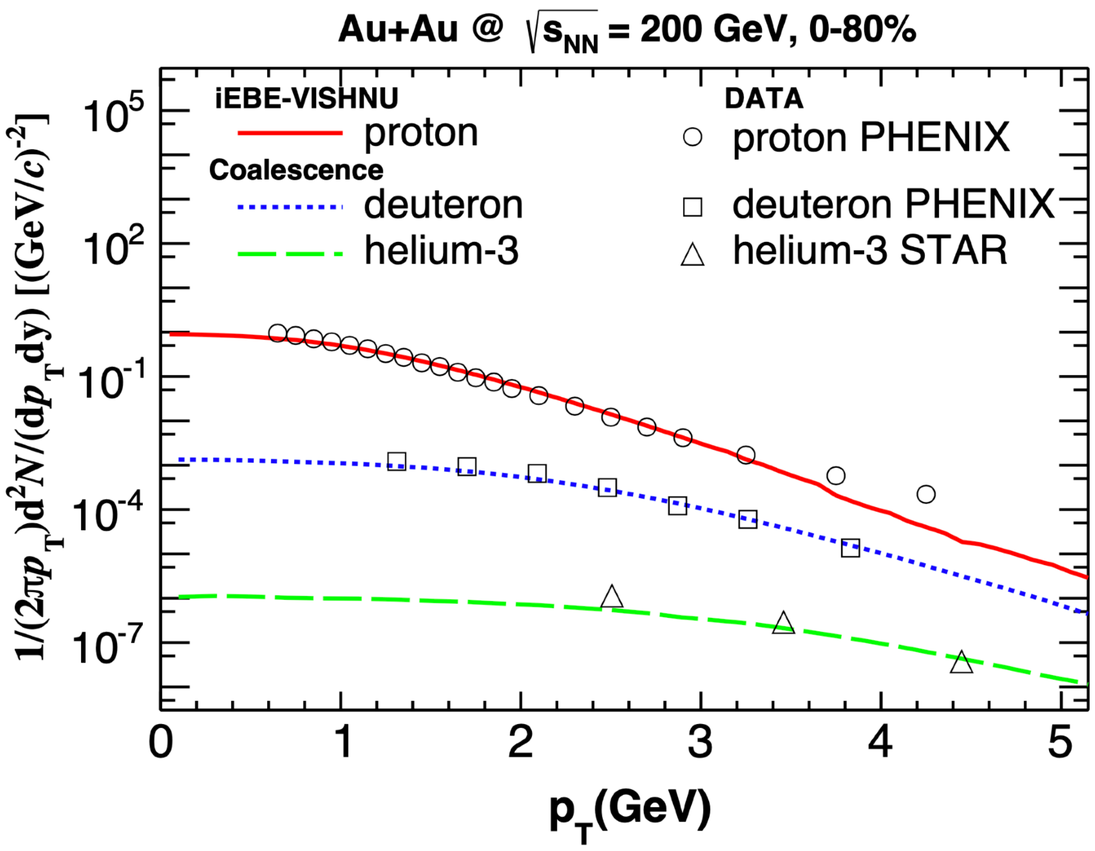

W. Zhao et al., PRC 98, 054905 (2018)

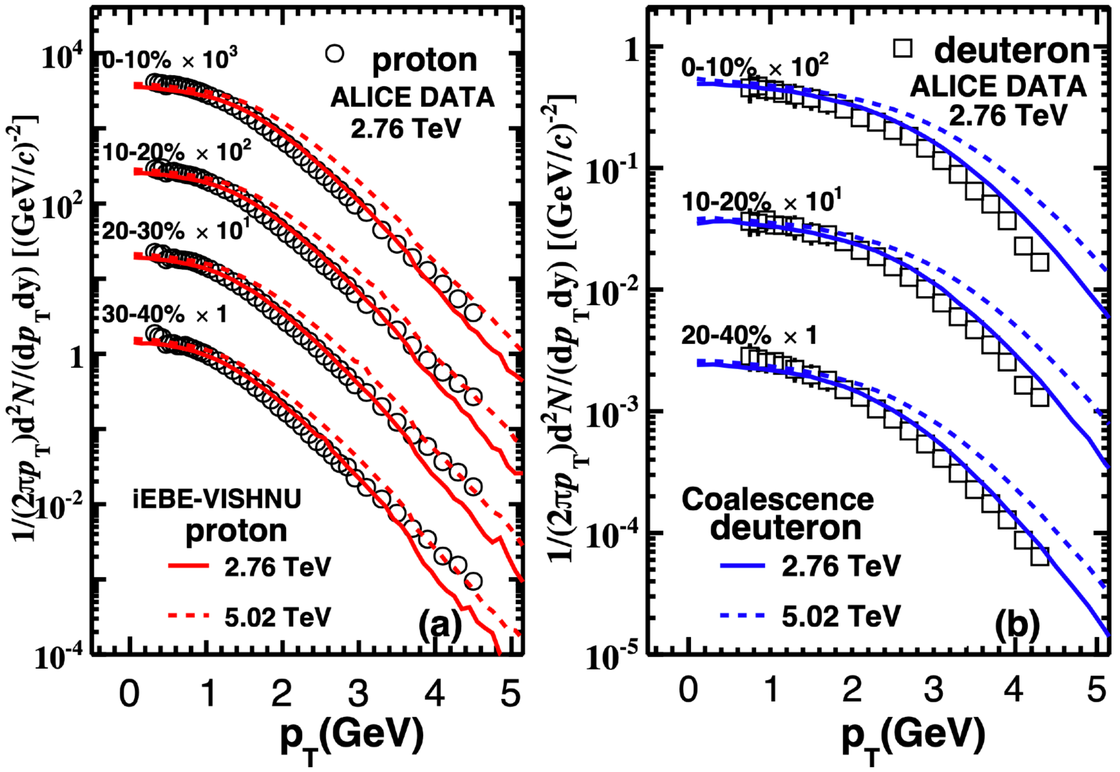

Coalescence model with phase space distributions of nucleons from iEBE-VISHNU

- AMPT initial conditions
- (1+2)d hydro (VISHNU) + UrQMD

Good description of deuteron p_T spectra both at RHIC and LHC energies

^{3}He p_T spectra vs. coalescence

W. Zhao et al., PRC 98, 054905 (2018)

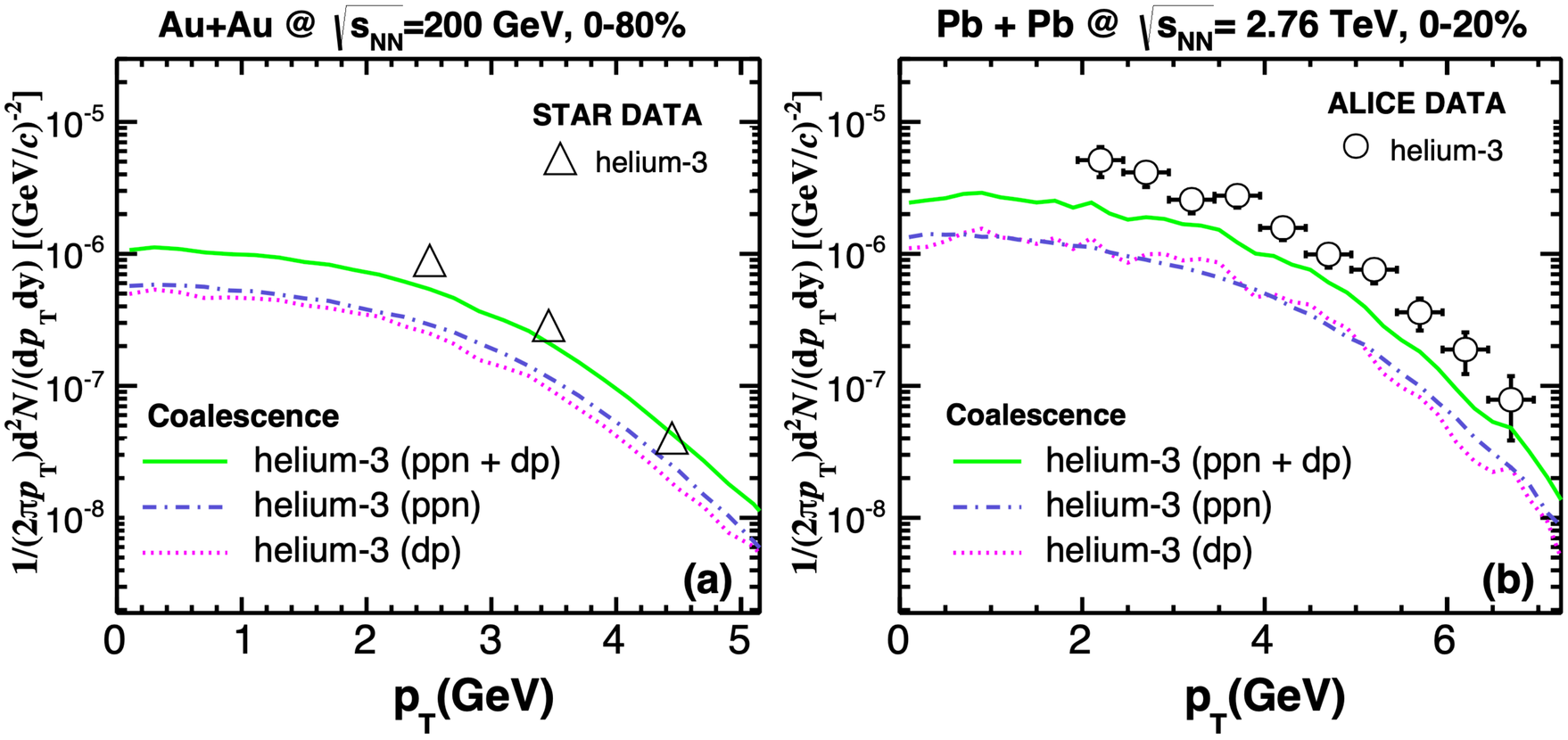

Description of the ^{3}He p_T spectrum from coalescence requires two contributions: two-body (d+p) and three-body coalescence (p+p+n)

- Good description of STAR data
- ALICE measurement underestimated by a factor 2

d/p and ^{3}He/p vs. multiplicity

d/p

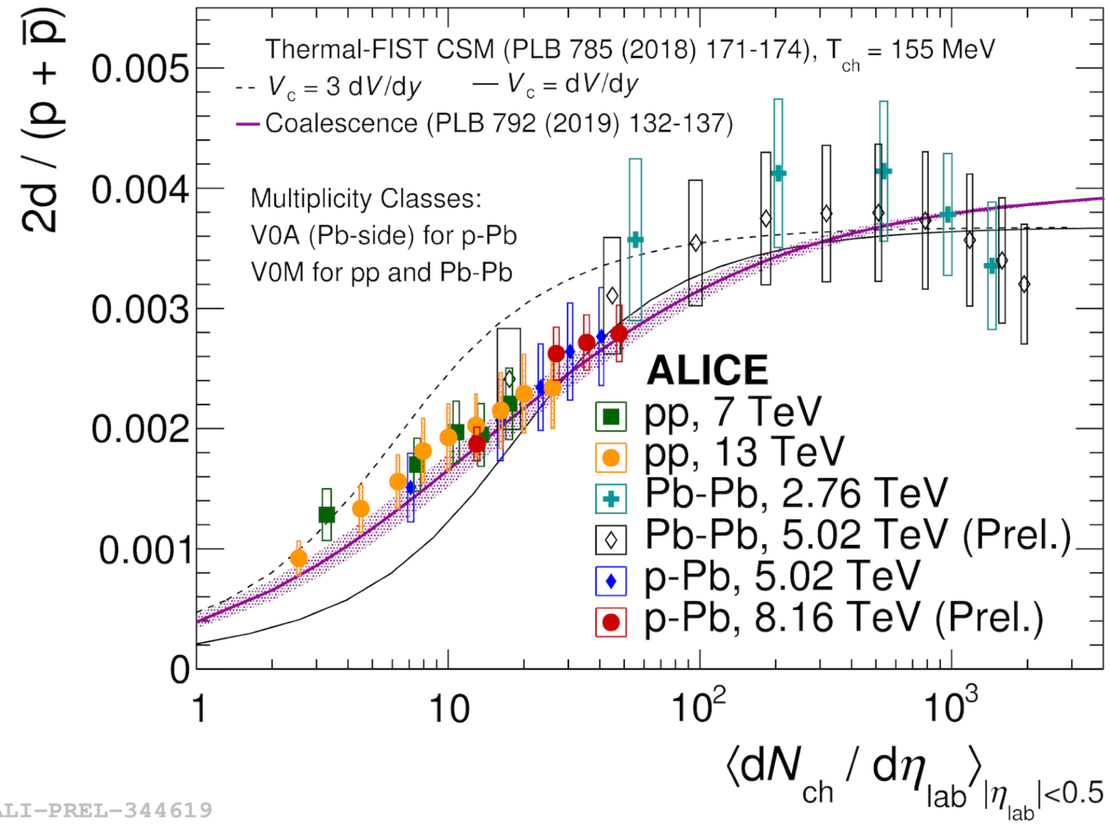

ALI-PREL-344619

^{3}He/p

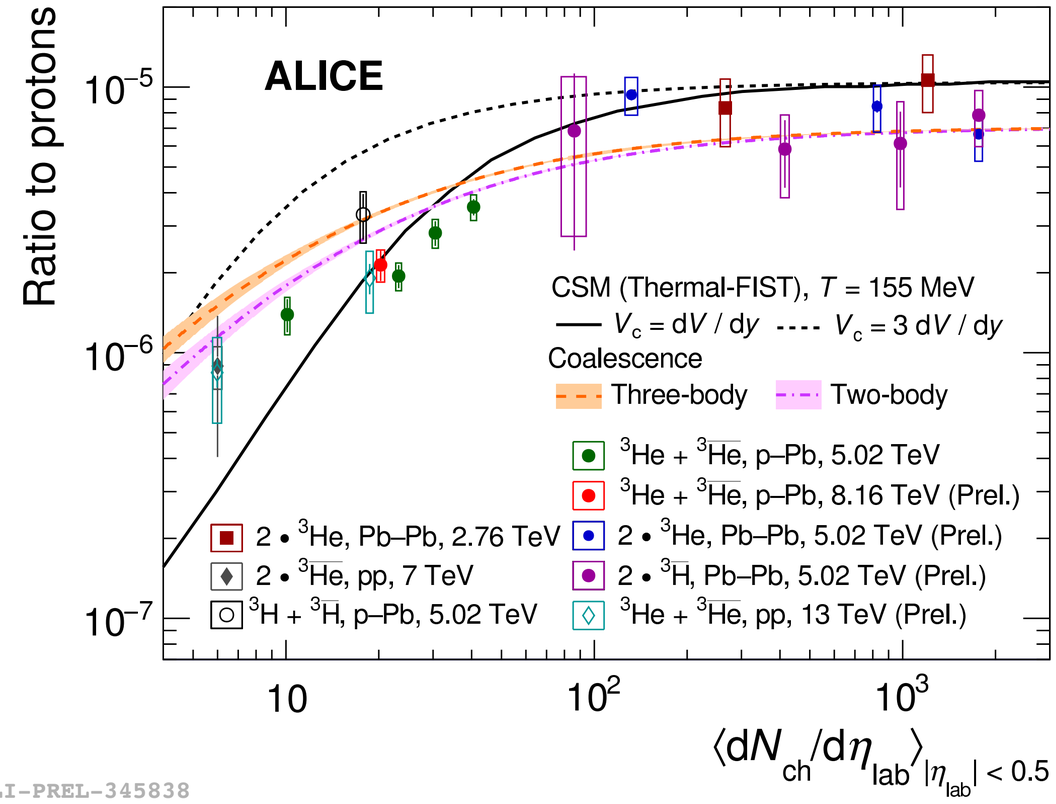

ALI-PREL-345838

Lower d/p and ^{3}He/p ratios in pp collisions → smooth transition towards grand-canonical limit

- d/p fairly well described by the coalescence model
- Tensions at intermediate multiplicities in ^{3}He/p for both CSM and coalescence

Coalescence parameter vs. multiplicity

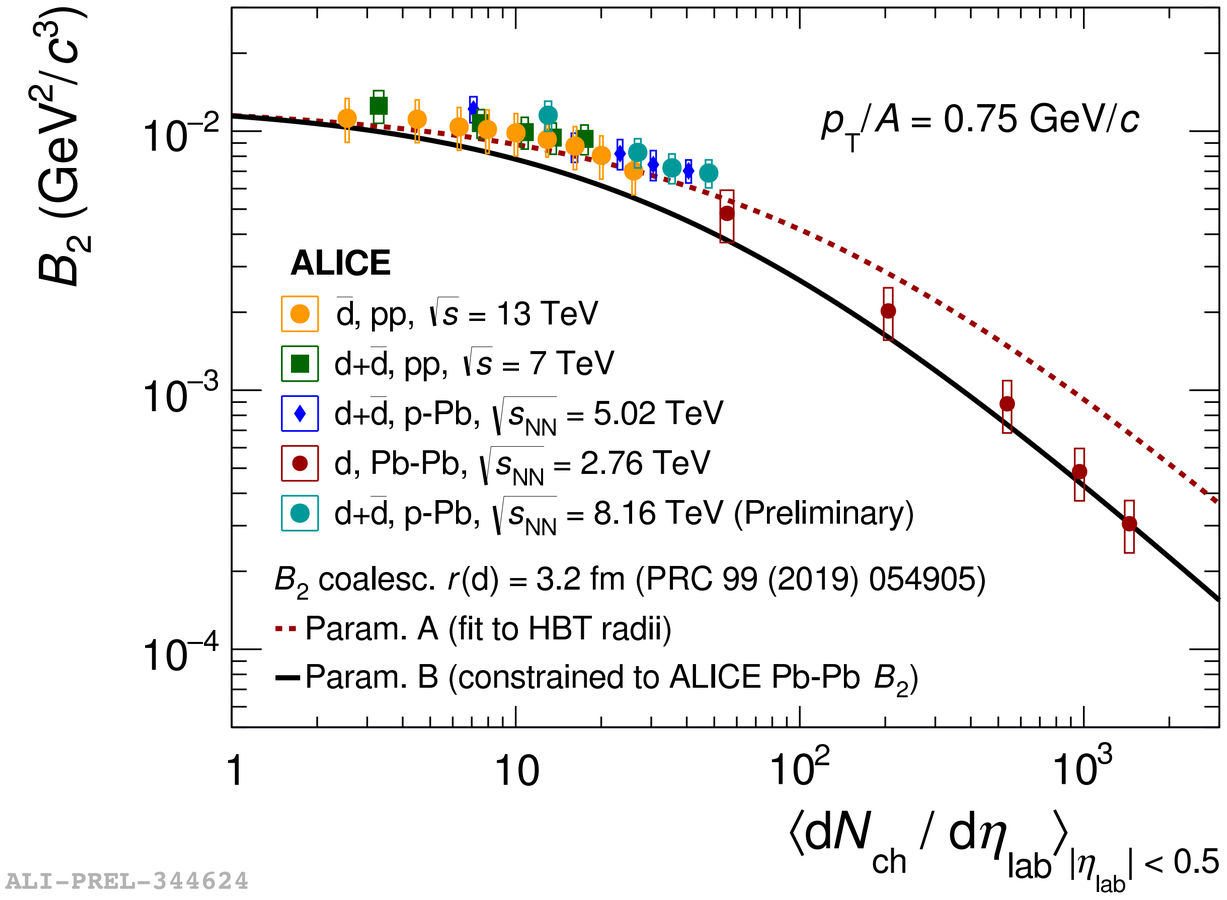

ALI-PREL-344624

Phys. Rev. C 99, 054905 (2019)

$$B_2 = \propto \frac{1}{R^3_{\text{source}}} \left[1 + \frac{r_d^2}{4R^2_{\text{source}}} \right]^{-3/2}$$

Radius of the particle-emitting source

Protons and neutrons with similar momenta have (on average) larger separation in larger systems

-> reduced coalescence probability

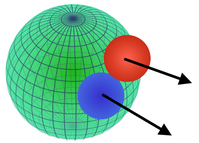

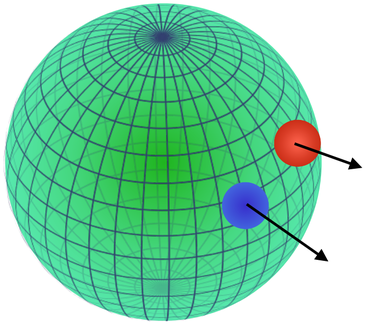

^{3}H/^{3}He vs. coalescence

Phys. Rev. C 101, 044906 (2020)

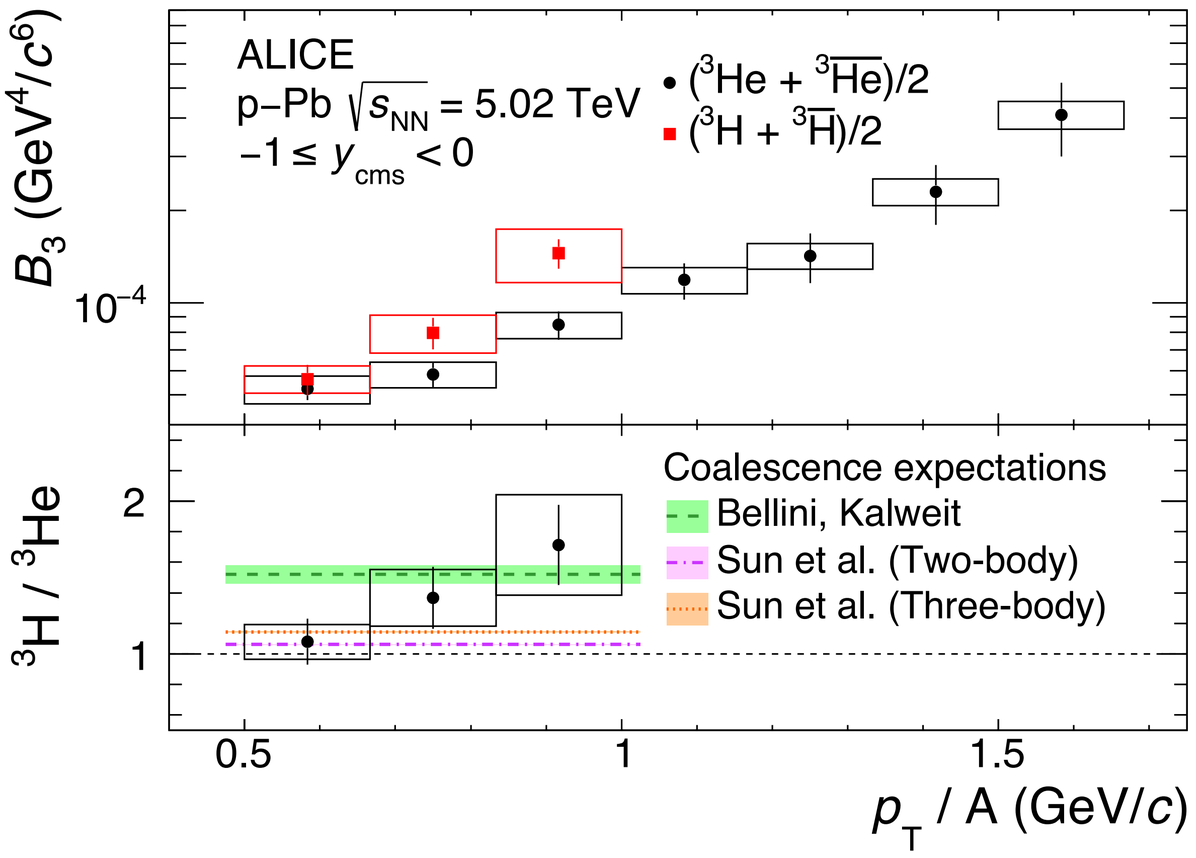

^{3}H and ^{3}He have similar masses but different radii (~15%)

- r (^{3}H) = 2.15 fm
- r (^{3}He) = 2.48 fm

Phys. Rev. C 99, 054905 (2019)

^{3}H/^{3}He in small systems sensitive to the production mechanism:

Thermal: $^3\mathrm{H}/^3\mathrm{He} \propto \exp\left(-\Delta M/T_{\mathrm{chem}}\right) \approx 1$

Coalescence: $^3\mathrm{H}/^3\mathrm{He} = \left[\dfrac{R^2_{\mathrm{source}} + r^2_{^3\mathrm{He}}/4}{R^2_{\mathrm{source}} + r^2_{^3\mathrm{H}}/4}\right]^3$

Existing data do not allow a conclusive statement

→ will be addressed in run3+4

Jet-associated deuteron production

Trigger particle
(p_T > 5 GeV/c) ≈ jet axis

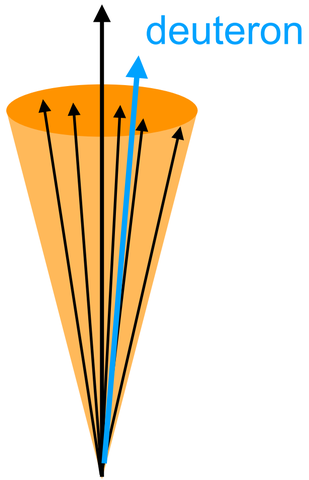

arXiv:2011.05898 [nucl-ex], submitted to PLB

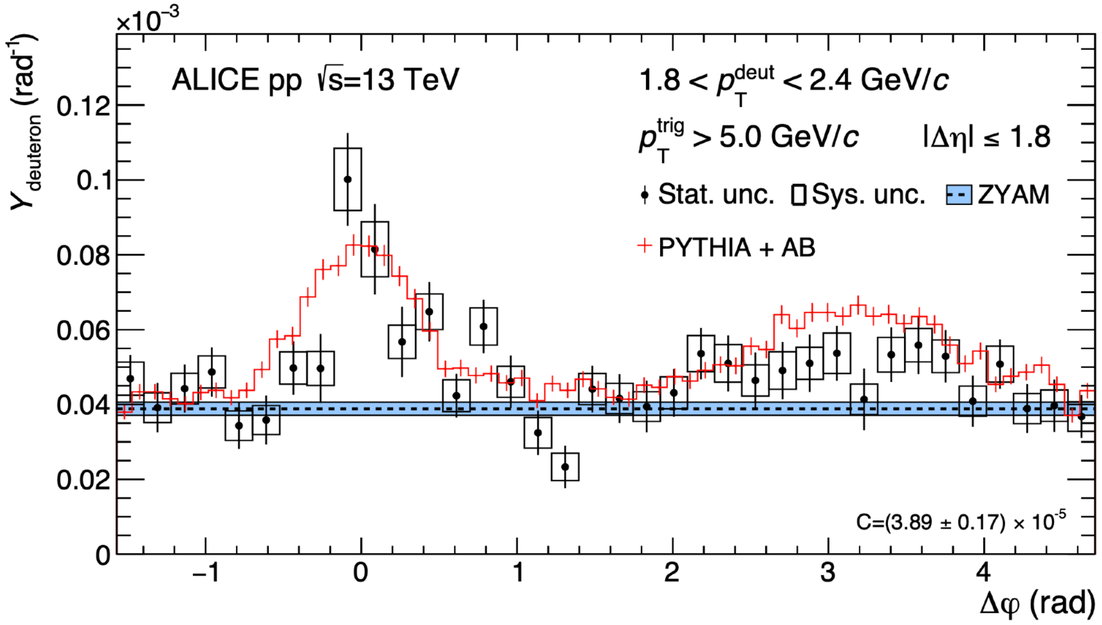

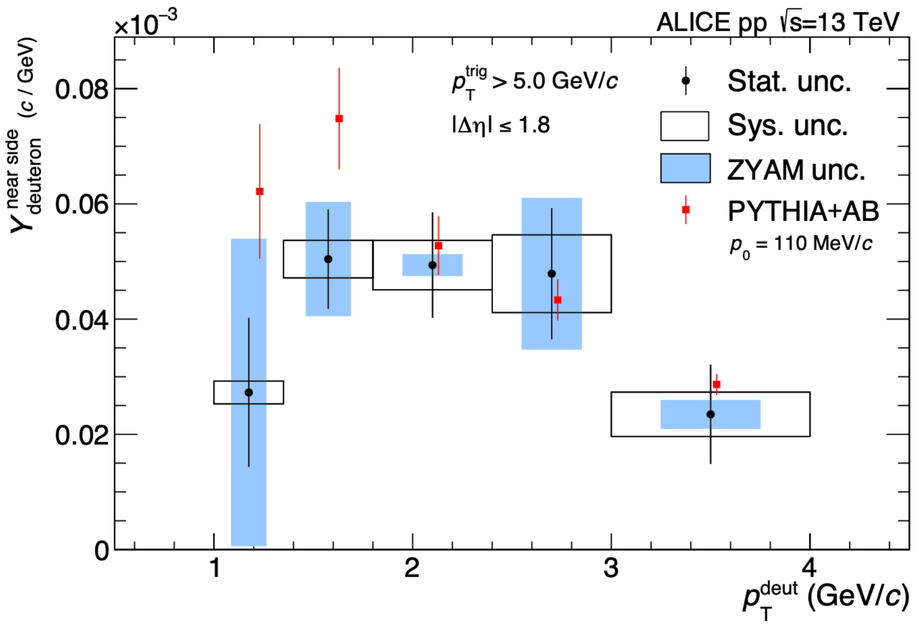

Significant near-side deuteron yield in $|\Delta\phi| < 0.7$ for p_T > 1.35 GeV/c

Results consistent with PYTHIA + coalescence (only momentum correlation)

Deuteron yield in jets ≈ 10-15% of deuterons in UE

Deuteron production vs. UE activity

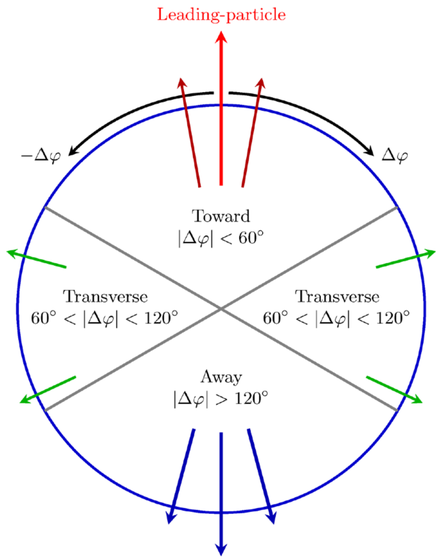

$$R_T = \frac{N_{ch}^T}{\langle N_{ch}^T \rangle}$$

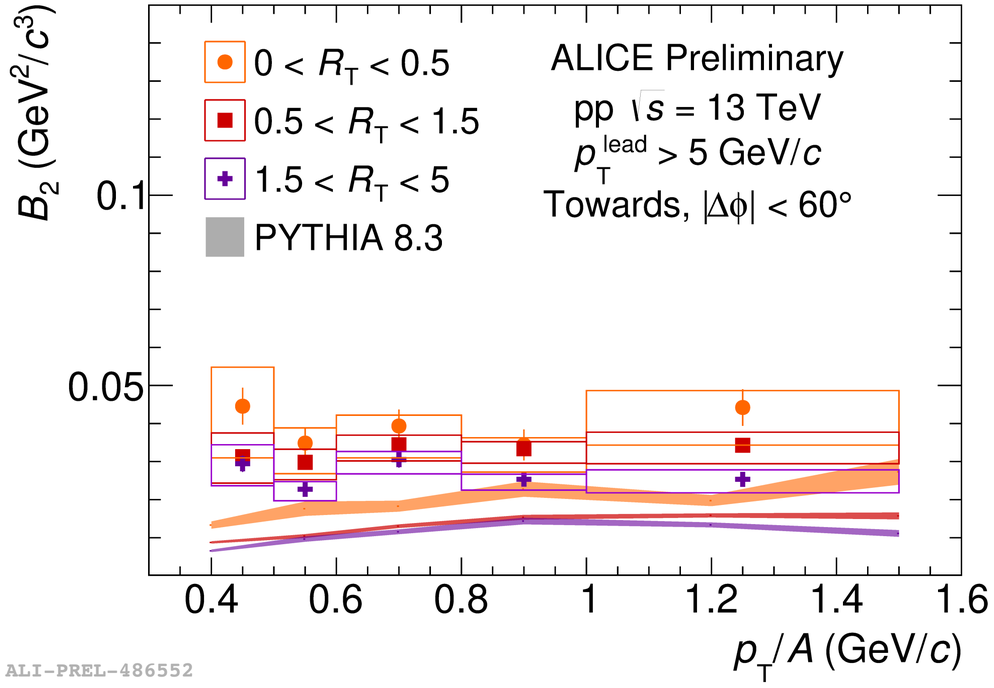

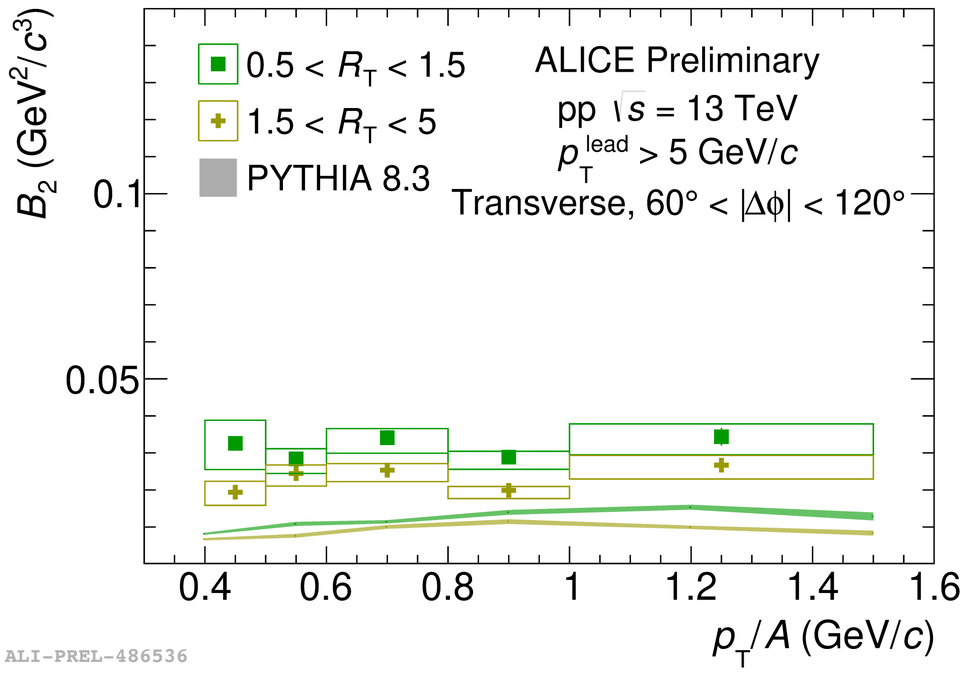

Similar B_2 in toward (jet+UE) and transverse (UE) regions for fixed R_T

- Hint of a larger B_2 in the toward region at low R_T (low UE activity)

PYTHIA 8.3 describes ordering and p_T dependence but not the magnitude

N.B. Deuterons in PYTHIA 8.3 produced using ordinary processes
$(NN \rightarrow d\pi, d\pi\pi, d\gamma)$ with parametrized cross sections → no coalescence

Hypertriton structure

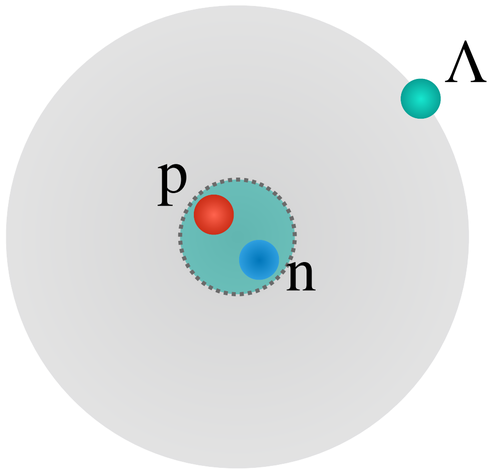

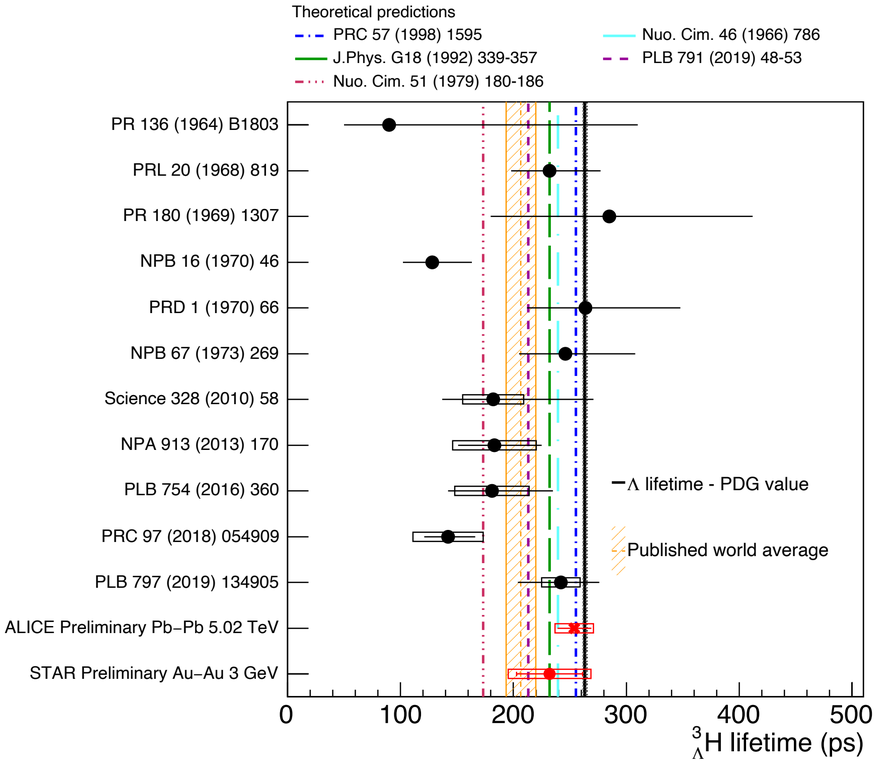

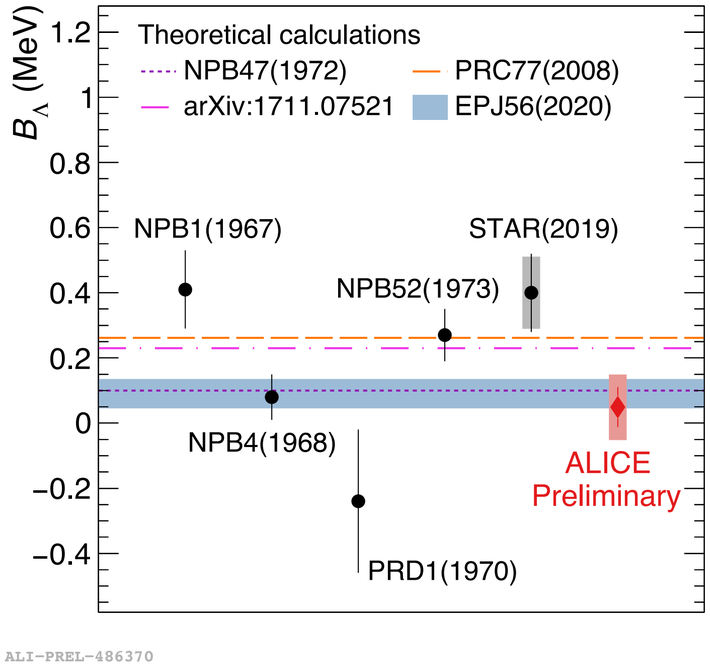

ALI-PREL-486370

Hypertriton lifetime very close to that of the Λ

- Most recent STAR result consistent with the ALICE measurement (puzzle solved? …)

$\tau_{^{3}_{\Lambda}\mathrm{H}} \approx \tau_{\Lambda}$ and small Λ separation energy indicate a loosely bound system with a halo structure:

"deuteron" core + Λ: $\sqrt{\langle r^2_{\Lambda-\mathrm{NN}'} \rangle} = 10.79^{+3.04}_{-1.53}$ fm **Phys. Rev. C 100, 034002 (2019)**

Hypernuclei production

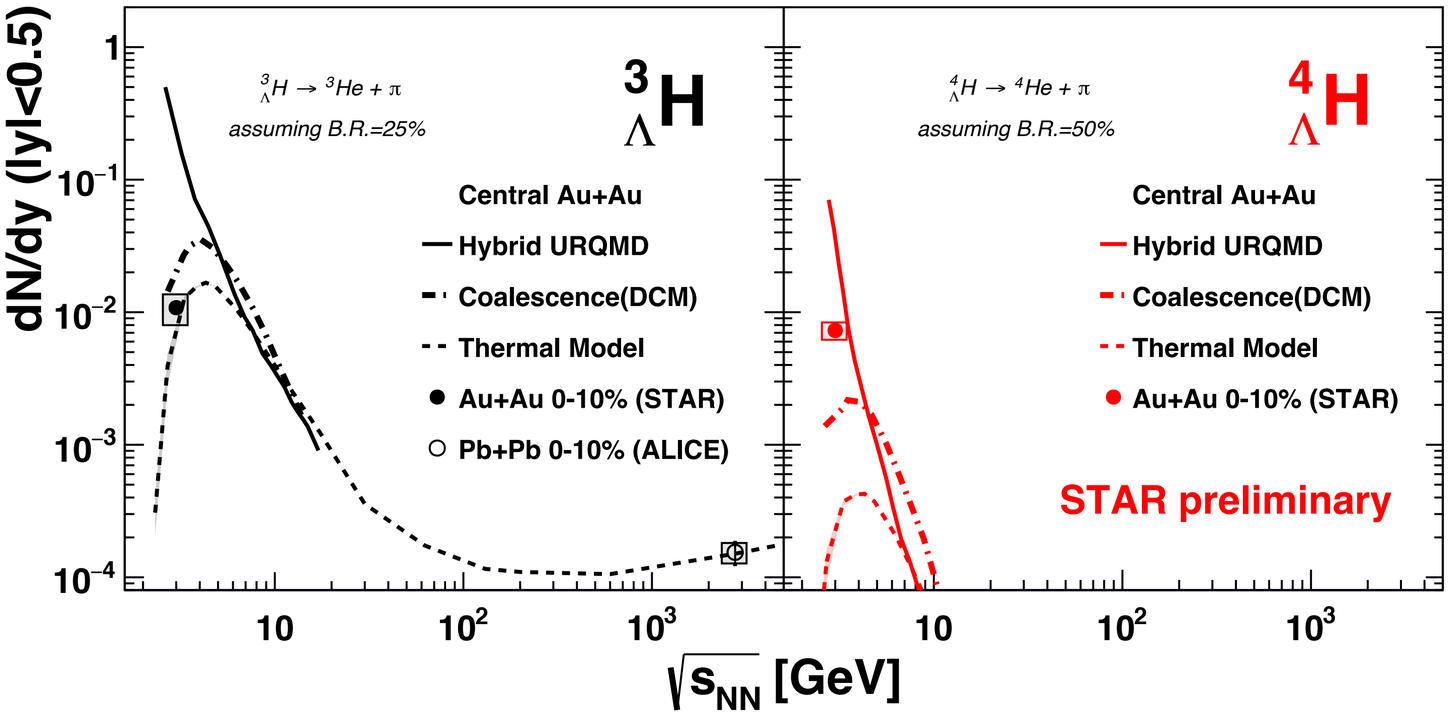

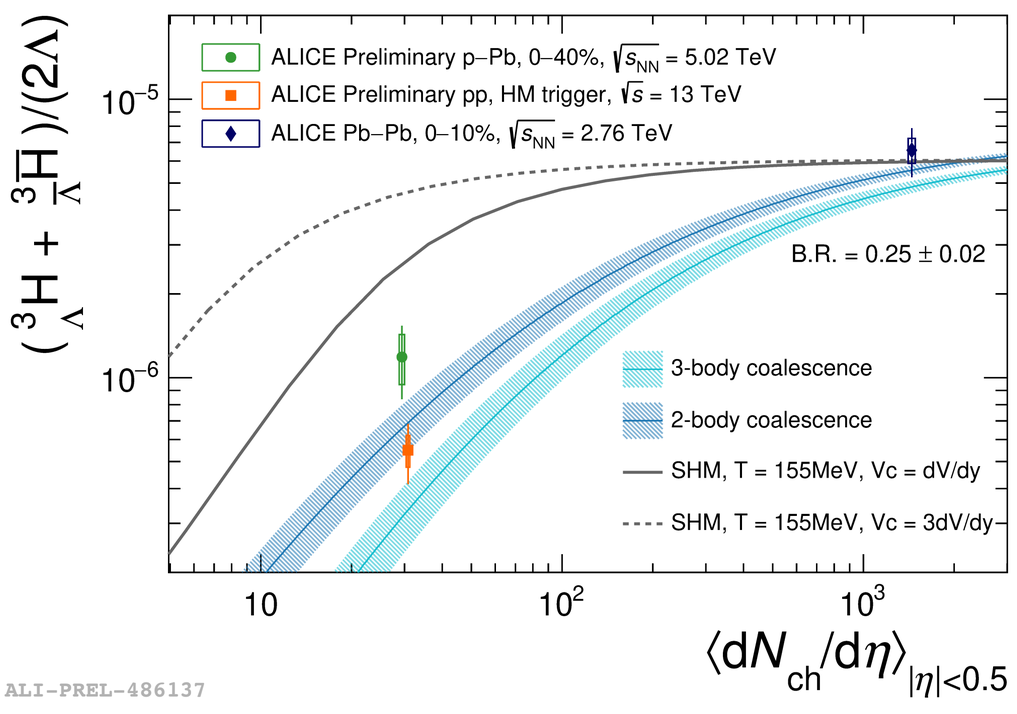

ALI-PREL-486137

- $^{3}_{\Lambda}\mathrm{H}$ yield measured in central AA collisions consistent with the thermal model
- $^{3}_{\Lambda}\mathrm{H}/\Lambda$ measured by ALICE in low-multiplicity collision systems favors coalescence model

  → Multiplicity dependence of $^{3}_{\Lambda}\mathrm{H}/\Lambda$ still needs to be explored: run3+4

The measurement of the $^{4}_{\Lambda}\mathrm{H}$ yield challenges the existing models

Summary

(Multi)strange hadron production:

- Dominant contribution to strange hadron yield from the underlying event
- Strangeness enhancement vs. multiplicity mostly driven by final-state multiplicity

Light (hyper)nuclei production:

- Hypertriton measurements from ALICE and STAR consistently indicate a weakly bound system with a halo structure: d+Λ
  $\rightarrow$ **consolidated result**
- Measurements of more complex (hyper)nuclei challenge the existing models

Thank you for your attention!

Backup slides

Ropes hadronization

Phys. Rev. D 100, 074023 (2019)

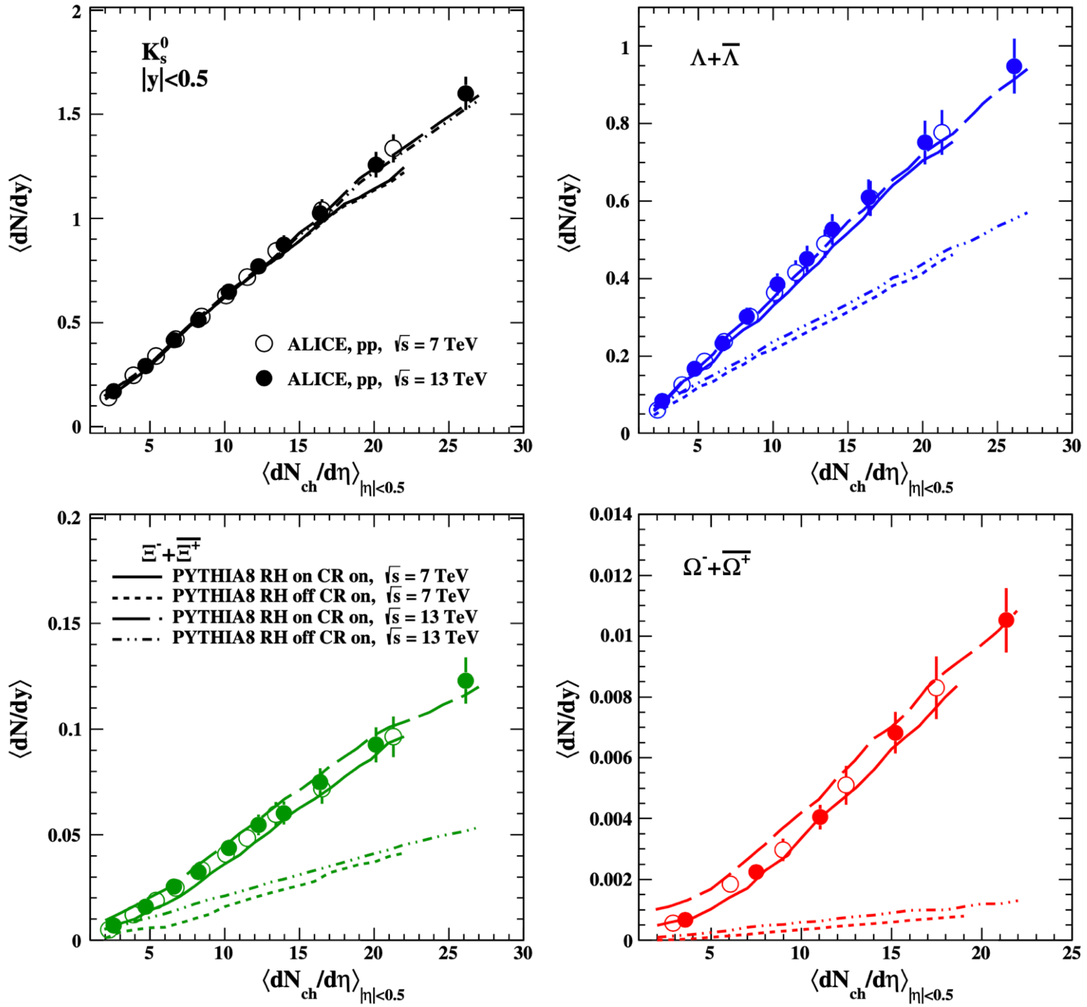

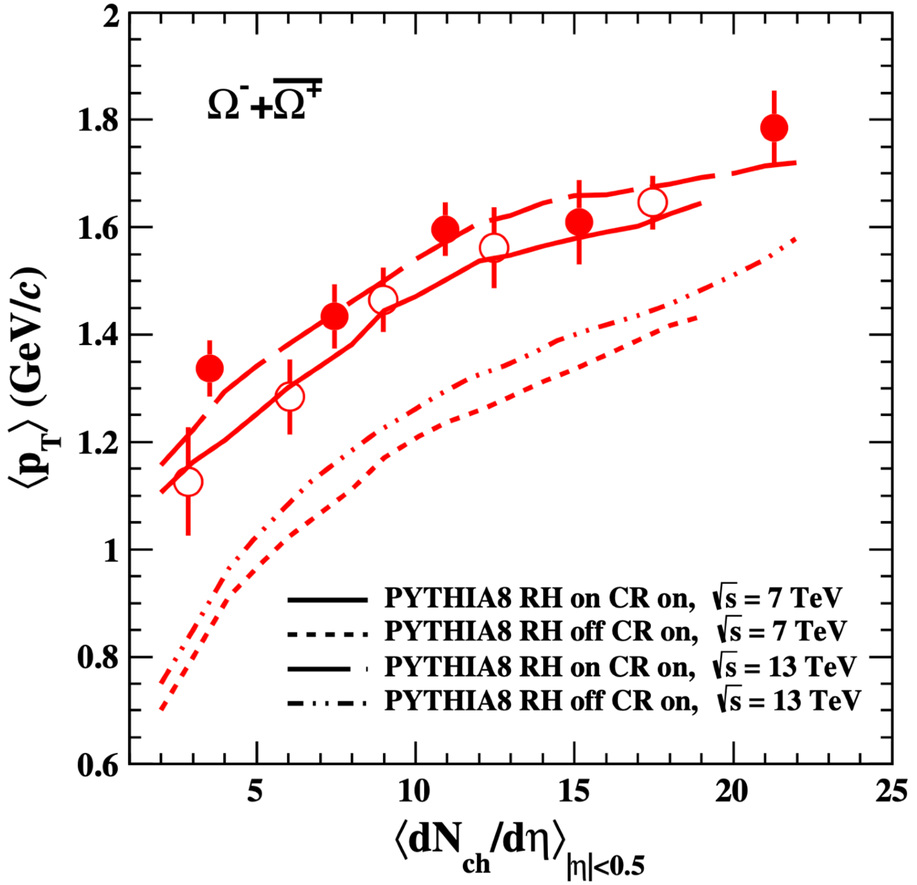

Rope hadronization mechanism successful in the description of strange hadron yields and $\langle p_T \rangle$ vs. multiplicity

Strangeness vs. UE activity

Leading particle:
highest p_T and p_T > 5 GeV/c

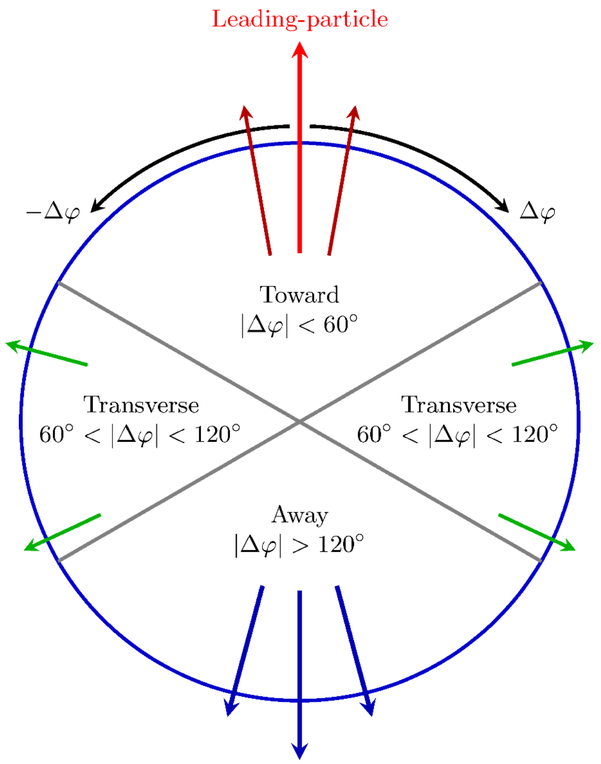

Toward region: jet + UE
Transverse region: UE
Away region: recoil jet + UE

JHEP 04, 192 (2020)

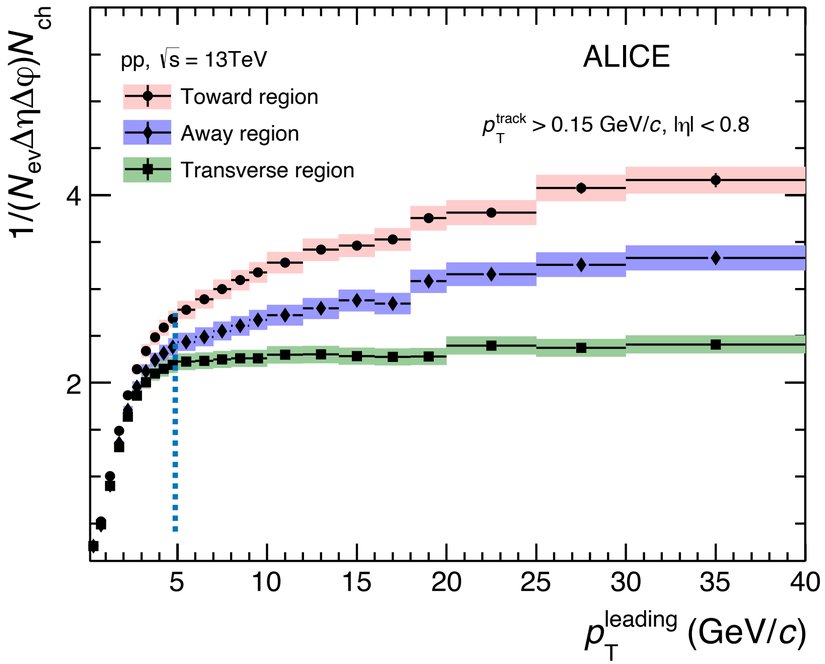

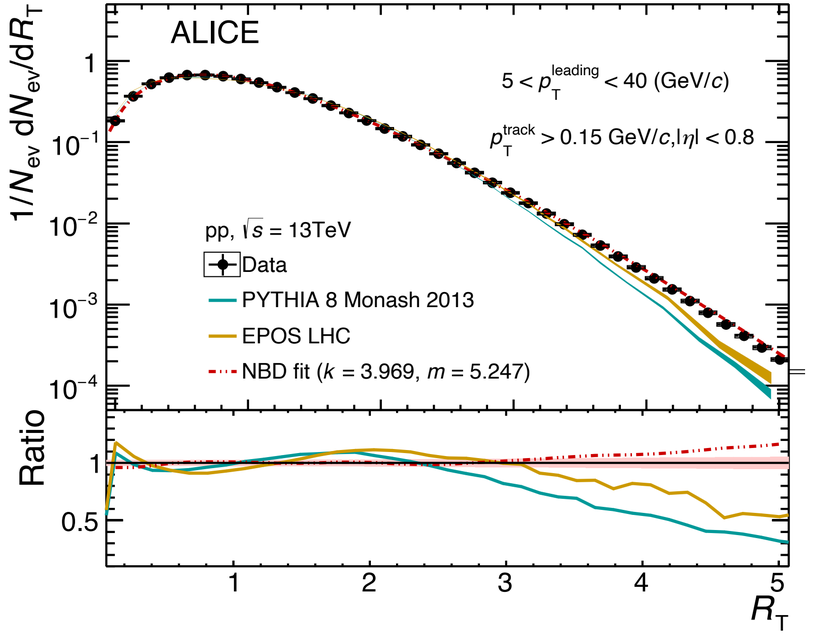

Charged particle density in the transverse region reaches a plateau for p_T > 5 GeV/c (MPI saturation)

Multiplicity in the transverse region as classifier for the UE activity

$$R_T = \frac{N_{ch}^T}{\langle N_{ch}^T \rangle}$$

R_T < 1: low UE activity
R_T > 1: high UE activity

Strangeness vs. UE activity

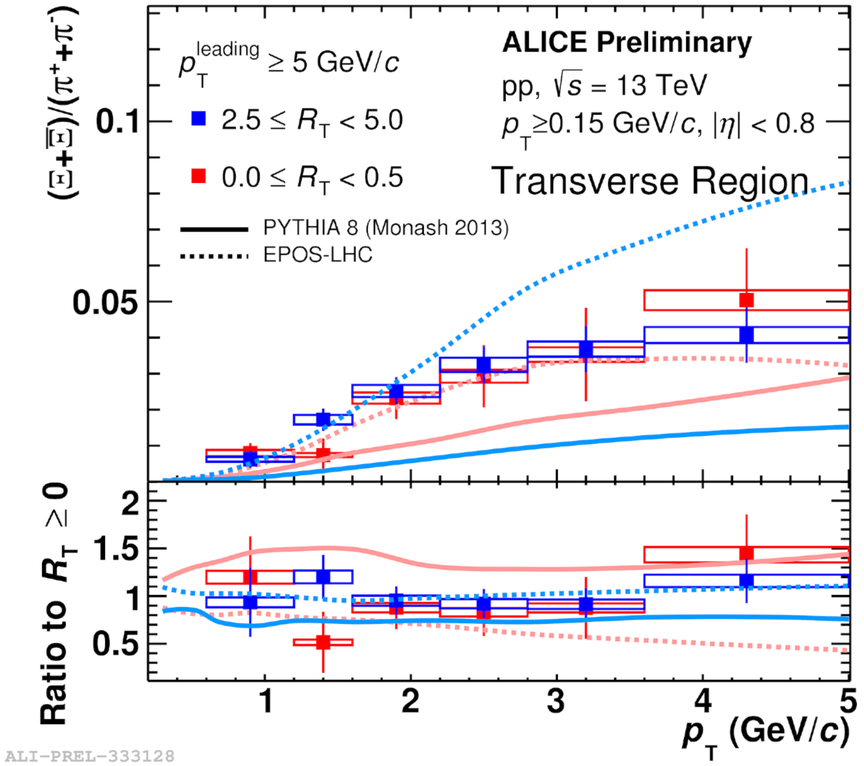

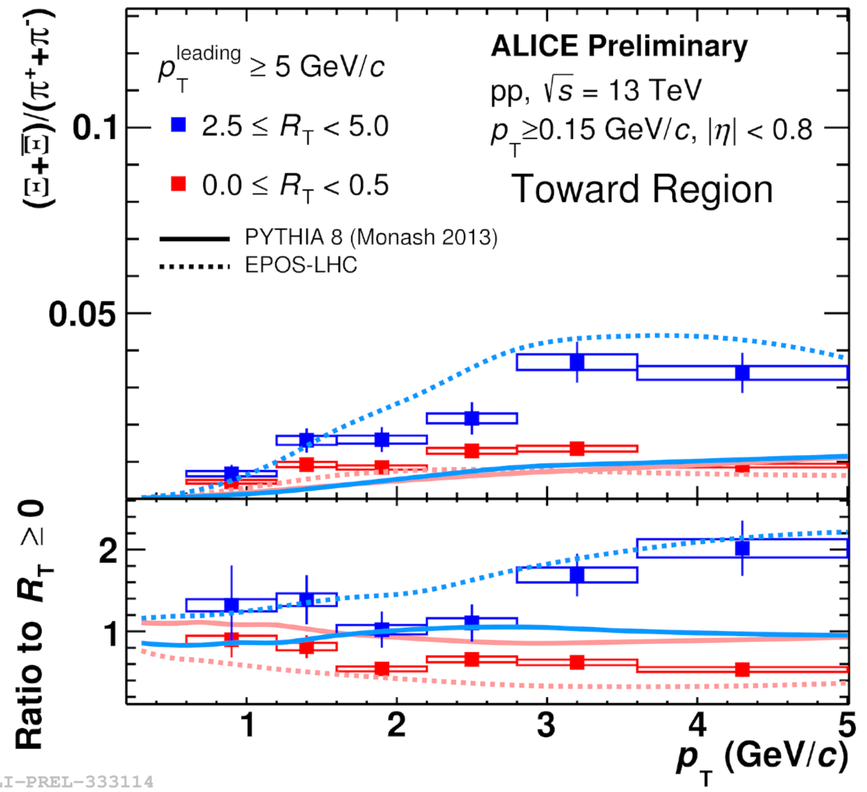

- Ξ/π does not significantly depend on R_T in the Transverse Region (UE)
- Ξ/π increases with R_T in the Toward Region (Jet + UE), approaching the values of the Transverse Region for high R_T

  → Ξ/π higher in the UE than in the jet